

Electron Interactions With $c\text{-C}_4\text{F}_8$

L. G. Christophorou^{a)} and J. K. Olthoff^{b)}

Electricity Division, Electronics and Electrical Engineering Laboratory, National Institute of Standards and Technology,
Gaithersburg, Maryland 20899-8113

(Received 29 January 2001; accepted 26 March 2001)

The limited electron collision cross-section and transport-coefficient data for the plasma processing gas perfluorocyclobutane ($c\text{-C}_4\text{F}_8$) are synthesized, assessed, and discussed. These include cross sections for total electron scattering, differential elastic electron scattering, partial and total ionization, dissociation into neutral fragments, and electron attachment, as well as data on electron transport, ionization, and attachment coefficients. The available data on both the electron collision cross sections and the electron transport coefficients require confirmation. Also, measurements are needed of the momentum transfer and elastic integral cross sections, and of the cross sections for other significant low-energy electron collision processes such as vibrational and electronic excitation. In addition, electron transport data over a wider range of values of the density-reduced electric field are needed. The present assessment of data on electron affinity, attachment, and scattering suggests the existence of negative ion states near -0.6 , 4.9 , 6.9 , 9.0 , and 10.5 eV. © 2001 by the U.S. Secretary of Commerce on behalf of the United States. All rights reserved.

Key words: attachment; $c\text{-C}_4\text{F}_8$; coefficients; cross sections; electron interactions; electron transport; ionization; perfluorocyclobutane; scattering.

Contents

1. Introduction.	450
2. Structural and Electronic Properties.	451
3. Electron Scattering Cross Sections.	451
3.1. Total electron scattering cross section, $\sigma_{\text{sc,t}}(\epsilon)$	451
3.2. Differential elastic electron scattering cross sections, $\sigma_{\text{e,diff}}$	455
3.3. Differential vibrational excitation cross section, $\sigma_{\text{vib,diff}}(\epsilon)$	455
4. Electron Impact Ionization.	455
4.1. Partial ionization cross sections, $\sigma_{\text{i,partial}}(\epsilon)$	455
4.2. Total ionization cross section, $\sigma_{\text{i,t}}(\epsilon)$	456
4.3. Density-reduced ionization coefficient, $\alpha/N(E/N)$	456
4.4. Density-reduced effective ionization coefficient, $(\alpha - \eta)/N(E/N)$	458
5. Dissociation into Neutral Fragments.	459
6. Electron Attachment.	461
6.1. Electron beam determined total electron attachment cross section $\sigma_{\text{a,t}}(\epsilon)$	461
6.2. Total electron attachment rate constant as a function of E/N , $k_{\text{a,t}}(E/N)$	465
6.3. Total electron attachment rate constant as a function of the mean electron energy, $k_{\text{a,t}}(\langle\epsilon\rangle)$	465
6.4. Swarm-unfolded total electron attachment cross section, $\sigma_{\text{a,t}}(\epsilon)$	466
6.5. Comparison of the values of $\sigma_{\text{a,t}}(\epsilon)$ derived from electron swarm and electron beam experiments.	466
6.6. Thermal value, $(k_{\text{a,t}})_{\text{th}}$, of the total electron attachment rate constant.	468
6.7. Total electron attachment rate constant as a function of the mean electron energy and gas temperature, $k_{\text{a,t}}(\langle\epsilon\rangle, T)$	468
6.8. Density-reduced electron attachment coefficient, $\eta/N(E/N)$	468
7. Electron Transport.	469
7.1. Electron drift velocity, $w(E/N)$	469
7.2. Ratio of the lateral electron diffusion coefficient to electron mobility, $D_{\text{T}}/\mu(E/N)$	469
8. Ion-Molecule Reactions.	469
9. Summary of Cross Sections and Rate Coefficients	471
10. Data Needs.	471
11. Acknowledgments.	471
12. References.	471

List of Tables

1. Definition of symbols.	451
2. Physical and structural data on the $c\text{-C}_4\text{F}_8$ molecule.	452

^{a)}Electronic mail: loucas.christophorou@nist.gov

^{b)}Electronic mail: james.olthoff@nist.gov

© 2001 by the U.S. Secretary of Commerce on behalf of the United States.
All rights reserved.

3. Negative ion states of $c\text{-C}_4\text{F}_8$	453	techniques	465
4. Suggested values for the total electron scattering cross section, $\sigma_{\text{sc,t}}(\epsilon)$, of $c\text{-C}_4\text{F}_8$	456	11. Relative cross sections for the formation of negative ions by electron attachment to $c\text{-C}_4\text{F}_8$..	465
5. Differential elastic electron scattering cross sections, $\sigma_{\text{e,diff}}$, for $c\text{-C}_4\text{F}_8$	458	12. Total electron attachment rate constant, $k_{\text{a,t}}(E/N)$, as a function of E/N for $c\text{-C}_4\text{F}_8$	465
6. Partial ionization cross sections, $\sigma_{\text{i,partial}}(\epsilon)$, of $c\text{-C}_4\text{F}_8$	459	13. Total electron attachment rate constant, $k_{\text{a,t}}(\langle\epsilon\rangle)$, as a function of $\langle\epsilon\rangle$ for $c\text{-C}_4\text{F}_8$	466
7. Partial ionization cross sections, $\sigma_{\text{i,partial}}(\epsilon)$, of $c\text{-C}_4\text{F}_8$	461	14. Swarm-determined total electron attachment cross section, $\sigma_{\text{a,t}}(\epsilon)$, of $c\text{-C}_4\text{F}_8$	466
8. Energy thresholds for the appearance of positive-ion fragments by electron impact on $c\text{-C}_4\text{F}_8$	462	15. Comparison of electron swarm and electron beam data for the total electron attachment cross section, $\sigma_{\text{a,t}}(\epsilon)$, of $c\text{-C}_4\text{F}_8$	467
9. Suggested values for the total ionization cross section, $\sigma_{\text{i,t}}(\epsilon)$, of $c\text{-C}_4\text{F}_8$	462	16. Total electron attachment rate constant as a function of $\langle\epsilon\rangle$ and T , $k_{\text{a,t}}(\langle\epsilon\rangle, T)$, for $c\text{-C}_4\text{F}_8$..	469
10. Values of the density-reduced ionization coefficient, $\alpha/N(E/N)$, for $c\text{-C}_4\text{F}_8$ derived from a fit to the data of Naidu <i>et al.</i> ⁷⁰	462	17. Density-reduced electron attachment coefficient, $\eta/N(E/N)$, for $c\text{-C}_4\text{F}_8$	469
11. Cross sections, $\sigma_{\text{dis,partial}}(\epsilon)$, for electron-impact dissociation of $c\text{-C}_4\text{F}_8$ into neutral fragments. ...	464	18. Electron drift velocity, $w(E/N)$, for $c\text{-C}_4\text{F}_8$	470
12. Autodetachment lifetime of $c\text{-C}_4\text{F}_8^{*-}$	464	19. Ratio of the lateral electron diffusion coefficient to electron mobility, $D_T/\mu(E/N)$, for $c\text{-C}_4\text{F}_8$...	470
13. Peak cross section values for negative ion fragments formed by electron impact on $c\text{-C}_4\text{F}_8$..	465	20. Summary of suggested cross sections.....	471
14. Recommended values of the total electron attachment rate constant, $k_{\text{a,t}}(\langle\epsilon\rangle)$, for $c\text{-C}_4\text{F}_8$	466		
15. Suggested values of the total electron attachment cross section, $\sigma_{\text{a,t}}(\epsilon)$, of $c\text{-C}_4\text{F}_8$	468		
16. Thermal values, $(k_{\text{a,t}})_{\text{th}}$, of the total electron attachment rate constant for $c\text{-C}_4\text{F}_8$	468		
17. Values of $\eta/N(E/N)$ for $c\text{-C}_4\text{F}_8$ ($T=293$ K) derived from a fit to the data of Naidu <i>et al.</i> ⁷⁰	469		
18. Suggested room-temperature values of the electron drift velocity, $w(E/N)$, for $c\text{-C}_4\text{F}_8$	470		
19. Suggested values of $D_T/\mu(E/N)$ for $c\text{-C}_4\text{F}_8$ ($T=293$ K) derived from a fit to the data of Naidu <i>et al.</i> ⁷⁰	471		

List of Figures

1. Energy positions, E_{NIS} , of the negative ion states of $c\text{-C}_4\text{F}_8$ below 12 eV.....	454
2. Total electron scattering cross section, $\sigma_{\text{sc,t}}(\epsilon)$, of $c\text{-C}_4\text{F}_8$	455
3. Differential elastic electron scattering cross sections, $\sigma_{\text{e,diff}}$, of $c\text{-C}_4\text{F}_8$	457
4. Vibrational differential electron scattering cross sections, $\sigma_{\text{vib,diff}}(\epsilon)$, of $c\text{-C}_4\text{F}_8$	458
5. Partial ionization cross sections, $\sigma_{\text{i,partial}}(\epsilon)$, of $c\text{-C}_4\text{F}_8$	460
6. Total ionization cross section, $\sigma_{\text{i,t}}(\epsilon)$, of $c\text{-C}_4\text{F}_8$..	462
7. Density-reduced ionization coefficient, $\alpha/N(E/N)$, for $c\text{-C}_4\text{F}_8$	462
8. Density-reduced effective ionization coefficient, $(\alpha - \eta)/N(E/N)$, for $c\text{-C}_4\text{F}_8$	463
9. Partial cross sections, $\sigma_{\text{dis,partial}}(\epsilon)$, for electron-impact dissociation of $c\text{-C}_4\text{F}_8$ into neutral fragments	463
10. Total electron attachment cross section, $\sigma_{\text{a,t}}(\epsilon)$, of $c\text{-C}_4\text{F}_8$ measured using electron beam	

1. Introduction

Perfluorocyclobutane ($c\text{-C}_4\text{F}_8$) is a processing gas employed in plasma etching (e.g., see Refs. 1–7). Electron impact on $c\text{-C}_4\text{F}_8$ generates large quantities of CF_2 radicals, which in $c\text{-C}_4\text{F}_8$ plasmas form a polymer coating on silicon and account for the high etching selectivity of SiO_2 over Si by $c\text{-C}_4\text{F}_8$ plasmas.^{3,5–7} The $c\text{-C}_4\text{F}_8$ molecule also decomposes thermally above about 633 K,⁸ principally via the unimolecular decomposition reaction $c\text{-C}_4\text{F}_8 \rightarrow 2 \text{C}_2\text{F}_4$ (see Refs. 8, 9 and references cited therein), and thus CF_2 radicals may also be formed in a $c\text{-C}_4\text{F}_8$ plasma by electron-impact dissociation of the C_2F_4 byproduct. Consistent with this decomposition mechanism are infrared multiphoton dissociation studies^{10–13} of $c\text{-C}_4\text{F}_8$ which show that photodissociation occurs via the process $c\text{-C}_4\text{F}_8 + nh\nu \rightarrow 2 \text{C}_2\text{F}_4$.

Besides its use in plasma etching, $c\text{-C}_4\text{F}_8$ has many other applications ranging from its use in retinal detachment surgery,^{14,15} to its possible utilization as a gaseous dielectric especially in gas mixtures.^{16–19} Perfluorocyclobutane is also of environmental interest because it is a global warming gas.²⁰ Its lifetime in the atmosphere, based on the assumption that photolysis is the dominant atmospheric loss process for $c\text{-C}_4\text{F}_8$, is very long (3200 yr).²⁰ However, Morris *et al.*²¹ argue that the atmospheric lifetime of $c\text{-C}_4\text{F}_8$ is significantly reduced (to 1400 yr) if consideration is given to its atmospheric removal by electron interactions. The long atmospheric lifetime of $c\text{-C}_4\text{F}_8$ partly accounts for its high global warming potential, which over a 100-yr time period is 8700 times that of CO_2 .²⁰

In this paper a number of collision cross sections, coefficients, and rate constants are used to quantify the various processes which result from collisions of low-energy (mostly less than 100 eV) electrons with the $c\text{-C}_4\text{F}_8$ molecule. These physical quantities are identified in Table 1 along with the

corresponding symbols and units. The procedure for assessing and recommending data followed in this paper is the same as in the previous nine papers in this series.²²⁻³⁰ Few of the available data sufficiently meet the assessment criteria^{22,25} to be "recommended," but suggested data are presented where possible. There is a need for further measurements on most of the electron collision cross sections and coefficients.

Besides the experimental data summarized, assessed, and discussed in this paper, there has been no published review and/or assessment of the data on the electron collision cross sections and electron transport coefficients for this molecule. There have been however two Boltzmann-code calculations^{31,32} of various coefficients, but these results are not discussed in this paper due to their unknown uncertainty.

2. Structural and Electronic Properties

Electron diffraction studies³³⁻³⁸ have shown that the carbon atoms in the *c*-C₄F₈ molecule are not planar. Similarly, infrared studies³⁹⁻⁴² are consistent with a nonplanar molecular structure. The *c*-C₄F₈ molecule has a puckered structure and belongs to the *D*_{2d} symmetry point group. Table 2 lists information on its structural properties and also values of the electron affinity, ionization threshold energy, dissociation energy, and polarizability of the *c*-C₄F₈ molecule.

The *c*-C₄F₈ molecule forms parent negative ions below ~1 eV and this property is consistent with the molecule having a positive electron affinity (EA). Besides the "zero-energy" electron attachment process which is associated with the negative ion state located at -EA, fragment negative ions are formed via a number of negative ion states which lie between 0 and ~12 eV. The energy positions of these negative ion states as indicated by the experimental data on nega-

tive ion formation are listed in Table 3 and plotted in Fig. 1. The similar results obtained from electron scattering experiments are also listed in Table 3 and plotted in Fig. 1. In the last column of Fig. 1 are shown the suggested energy positions of the lowest negative ion states of *c*-C₄F₈: -0.62, 4.9, 6.9, 9.0, and 10.5 eV. These suggested values were determined as follows: The value -0.62 eV is the average of the highest two electron affinity values listed in Table 2. The third (lower) value was not considered since it is only a lower limit. The 4.9 and 9.0 eV values are those from electron scattering experiments, which are expected to lie somewhat higher than the corresponding values determined from dissociative electron attachment experiments. The 6.9 and the 10.5 eV values are averages of values measured by various groups (see Table 3) for the energies at which the cross section for F⁻ production by electron attachment exhibits a maximum.

3. Electron Scattering Cross Sections

3.1. Total electron scattering cross section, $\sigma_{\text{sc,t}}(\epsilon)$

There have been two recent measurements⁵⁷⁻⁵⁹ of the total electron scattering cross section $\sigma_{\text{sc,t}}(\epsilon)$ of *c*-C₄F₈ which are compared in Fig. 2. The measurements of Sanabia *et al.*⁵⁷ cover the low-energy range from 1 to 20 eV and those of Nishimura^{58,59} cover a wider energy range from 2 to 3000 eV. Sanabia *et al.* did not quote the uncertainty of their data, but Nishimura gives the combined systematic and statistical uncertainties of his measurements to be between 2.8% and 5.9% depending on the electron energy. Representative error bars for the data of Nishimura are shown in Fig. 2. Generally, the data of Nishimura lie higher than those of Sanabia *et al.*⁵⁷

TABLE 1. Definition of symbols

Symbol	Definition	Common scale and units
$\sigma_{\text{sc,t}}(\epsilon)$	Total electron scattering cross section	10^{-16} cm^2 ; 10^{-20} m^2
$\sigma_{\text{e,diff}}$	Elastic differential electron scattering cross section	$10^{-16} \text{ cm}^2 \text{ sr}^{-1}$
$\sigma_{\text{vib,diff}}(\epsilon)$	Vibrational differential electron scattering cross section	$10^{-16} \text{ cm}^2 \text{ sr}^{-1}$
$\sigma_{\text{i,partial}}(\epsilon)$	Partial ionization cross section	10^{-16} cm^2 ; 10^{-20} m^2
$\sigma_{\text{it}}(\epsilon)$	Total ionization cross section	10^{-16} cm^2 ; 10^{-20} m^2
$\sigma_{\text{dis,partial}}(\epsilon)$	Partial cross section for dissociation into neutrals	10^{-18} cm^2 ; 10^{-22} m^2
$\sigma_{\text{a,t}}(\epsilon)$	Total electron attachment cross section	10^{-15} cm^2 ; 10^{-19} m^2
$\sigma_{\text{da,t}}(\epsilon)$	Total dissociative electron attachment cross section	10^{-16} cm^2 ; 10^{-20} m^2
$\alpha/N(E/N)$	Density-reduced ionization coefficient	10^{-18} cm^2 or 10^{-22} m^2
$(\alpha - \eta)/N(E/N)$	Density-reduced effective ionization coefficient	10^{-18} cm^2 or 10^{-22} m^2
$k_{\text{a,t}}(E/N)$	Total electron attachment rate constant	$10^{-9} \text{ cm}^3 \text{ s}^{-1}$
$(k_{\text{a,t}})_{\text{th}}$	Thermal electron attachment rate constant	$10^{-9} \text{ cm}^3 \text{ s}^{-1}$
$\eta/N(E/N)$	Density-reduced electron attachment coefficient	10^{-17} cm^2 or 10^{-21} m^2
$w(E/N)$	Electron drift velocity	10^7 cm s^{-1}
$D_{\text{T}}/\mu(E/N)$	Ratio of lateral electron diffusion coefficient to electron mobility	V

TABLE 2. Physical and structural data on the $c\text{-C}_4\text{F}_8$ molecule

Physical quantity	Value	Reference	Method
Electron affinity	~ 0.63 eV	43	Electron attachment/detachment studies
	0.61 eV	44	Electron attachment
	≥ 0.4 eV	45	Endothermic negative-ion charge-transfer reactions
Ionization threshold energy	11.6 ± 0.2 eV	46	TPEPICO ^a spectroscopy
	12.1 ± 0.1 eV ^b	47	Electron impact
	12.23 eV ^c	48	
	12.25 eV ^d	49	Electron impact
Dissociation energy, D(C-F)	$\sim 4.4 \pm 0.2$ eV	47	Electron impact
Polarizability	73.7×10^{-25} cm ³	50	From data on liquid density and refractive index using the Lorenz-Lorentz equation.
	92.4×10^{-25} cm ³	50	Using ion cyclotron resonance data
	74.9×10^{-25} cm ³	50	Semiempirical calculation
	104.3×10^{-25} cm ³	50	Semiempirical calculation
	124.7×10^{-25} cm ³	50	Semiempirical calculation
Molecular structure^e parameters			
C-C internuclear distance	1.63 ± 0.02 Å	35	Electron diffraction
	1.60 ± 0.04 Å	34	Electron diffraction
	1.58 Å	38	Electron diffraction
	1.566 ± 0.008 Å	36	Electron diffraction
	1.560 ± 0.009 Å	37	Electron diffraction
	1.54 Å	33	Electron diffraction
C-F internuclear distance	1.38 Å	33	Electron diffraction
	1.333 ± 0.002 Å	36	Electron diffraction
	1.333 Å	38	Electron diffraction
	1.332 ± 0.005 Å	35	Electron diffraction
	1.33 ± 0.02 Å	34	Electron diffraction
	1.324 ± 0.005 Å	37	Electron diffraction
F-C-F angle	110°	38	Electron diffraction
	$109.9^\circ \pm 0.3^\circ$	36	Electron diffraction
	$109.5^\circ \pm 3^\circ$	34	Electron diffraction
	$109^\circ \pm 1^\circ$	37	Electron diffraction
	$108^\circ \pm 2^\circ$	35	Electron diffraction
C-C-C angle	$89.3^\circ \pm 0.3^\circ$	36	Electron diffraction
	$\sim 89^\circ$	34	Electron diffraction
	88.8°	38	Electron diffraction
Dihedral angle	$10^\circ \pm 3^\circ$	35	Electron diffraction
	$17.4^\circ \pm 0.3^\circ$	36	Electron diffraction

^aThreshold photoelectron-photoion coincidence technique.

^bThis is the value of the threshold energy for the formation of C_3F_5^+ , the lowest threshold value for the positive ions listed in Ref. 47.

^cVertical value.

^dThe same (lowest) value is listed for the "appearance" of C_3F_5^+ and C_2F_4^+ .

^eChang *et al.*³⁶ give the tilt angle for CF_2 to be -5.4° .

TABLE 3. Negative ion states of *c*-C₄F₈

Energy position (eV)	Type of measurement	Reference
~0.0	Nondissociative electron attachment	51
0.03 ^a (0.23) ^b	Nondissociative electron attachment	52, 47
0.4±0.08	Total electron attachment	53
0.45±0.1	Nondissociative electron attachment	54
1.75 ^a (1.9) ^b	Dissociative electron attachment producing F ⁻	47
1.75 ^a (1.9) ^b	Dissociative electron attachment producing C ₃ F ₅ ⁻	47
3.75 ^a (4.05) ^b	Dissociative electron attachment producing C ₃ F ₅ ⁻	47
4.1	Dissociative electron attachment producing C ₃ F ₅ ⁻	51
4.3	Dissociative electron attachment producing F ⁻	49
4.3 ^a (4.6) ^b	Dissociative electron attachment producing F ⁻	47
4.35 ^a	Dissociative electron attachment producing CF ₃ ⁻	47
4.35±0.1	Dissociative electron attachment producing C ₂ F ₅ ⁻	54
4.4 ^a	Dissociative electron attachment producing C ₂ F ₅ ⁻	47
4.5±0.08	Dissociative electron attachment producing F ⁻	53
4.8	Dissociative electron attachment producing F ⁻	51
4.8	Dissociative electron attachment producing CF ₃ ⁻	51
4.9	Dissociative electron attachment producing C ₂ F ₃ ⁻	51
4.95±0.1	Dissociative electron attachment producing F ⁻	54, 55
4.95±0.1	Dissociative electron attachment producing F ₂ ⁻	54
4.95±0.1	Dissociative electron attachment producing CF ₂ ⁻	54
4.95±0.1	Dissociative electron attachment producing CF ₃ ⁻	54, 55
5.0	Dissociative electron attachment producing CF ₃ ⁻	49
4.91	Derivative electron transmission spectrum	56
~6	Total electron scattering cross section	57
6.5	Dissociative electron attachment producing F ⁻	51
6.75 ^a (7.1) ^b	Dissociative electron attachment producing F ⁻	47
6.8	Dissociative electron attachment producing F ⁻	49
6.9±0.08	Dissociative electron attachment producing F ⁻	53
7.4±0.2	Dissociative electron attachment producing F ⁻	54, 55
7.9	Dissociative electron attachment producing F ⁻	51
7.9	Dissociative electron attachment producing C ₂ F ₃ ⁻	51
8.0	Dissociative electron attachment producing F ⁻	49
8.1±0.08	Dissociative electron attachment producing F ⁻	53
8.2 ^a (8.45) ^b	Dissociative electron attachment producing F ⁻	47
8.5±0.3	Dissociative electron attachment producing F ₂ ⁻	54
8.6±0.2	Dissociative electron attachment producing F ⁻	54, 55
8.8±0.1	Dissociative electron attachment producing CF ₂ ⁻	54
~9	Total electron scattering cross section	58, 59
~9	Total electron scattering cross section	57
10.2	Dissociative electron attachment producing F ⁻	51
10.3	Dissociative electron attachment producing F ⁻	49
10.4±0.08	Dissociative electron attachment producing F ⁻	53
10.4±0.3	Dissociative electron attachment producing F ₂ ⁻	54
10.5 ^a (10.8) ^b	Dissociative electron attachment producing F ⁻	47
10.8±0.2	Dissociative electron attachment producing F ⁻	54, 55
11.2±0.2	Dissociative electron attachment producing CF ₂ ⁻	54

^aCalibration made using the production of SF₆⁻ from SF₆ (peak at 0.0 eV).

^bCalibration made using the production of O⁻ from CO (peak at 9.8 eV).

The cross section of Sanabia *et al.*⁵⁷ shows a pronounced minimum at ~4 eV and it rises steeply as the energy is decreased below ~2 eV. This latter feature is consistent with a large electron attachment cross section near zero energy (see Sec. 6.4). The cross section of Sanabia *et al.* also indicates a minor enhancement near 6.0 eV, which is consistent with the existence of a negative ion resonance at 5.9 eV, as detected

in the derivative electron transmission spectrum⁵⁶ and in dissociative electron attachment studies near 5 eV (see Table 3). Both the cross section data of Sanabia *et al.* and Nishimura *et al.*^{58,59} show another cross section enhancement near 9 eV, which is in agreement with dissociative electron attachment studies indicating (see Table 3) a negative ion state at this energy. In addition, the data of Nishimura show "humps" at

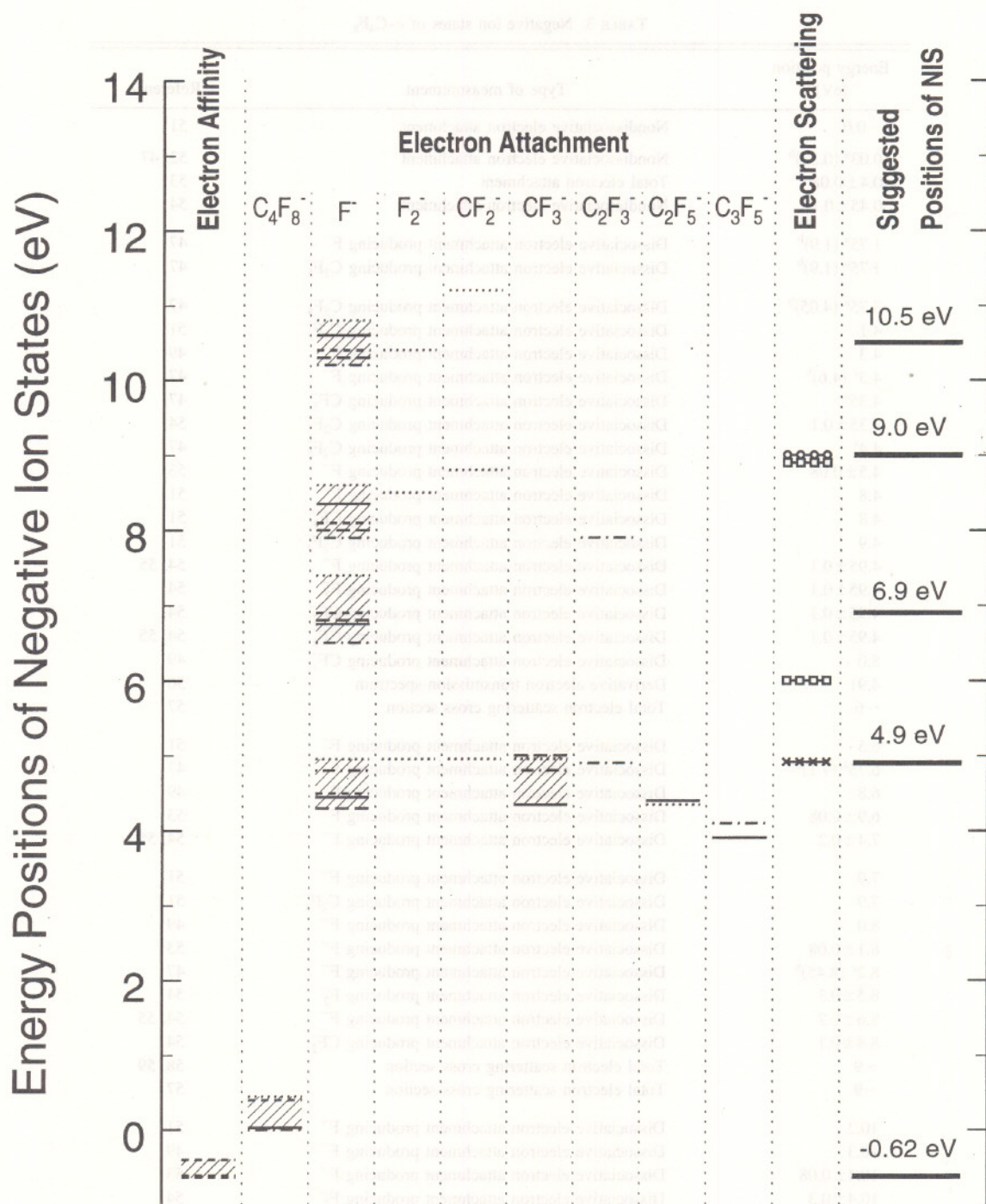


FIG. 1. Energy positions, E_{NIS} , of the negative ion states of *c*-C₄F₈ below 12 eV as obtained from electron affinity, electron attachment, and electron scattering studies. Electron affinity values: see Table 2 and the text. Electron attachment values: (···), Ref. 54; (—), Ref. 47; (- · -) Ref. 51; (- - -) Ref. 53; (- -) Ref. 49. Electron scattering values: (×-×) Ref. 56; (□-□) Ref. 57; (○-○) Refs. 58, 59. The peak at 1.75 eV observed in Ref. 47 for F⁻ and C₃F₅⁻ is not shown in the figure since it has not been reproduced by any of the other studies.

about 20 and 40 eV. These energies are outside the energy region where cross-section enhancements due to negative ion states are normally expected.

The disparity between the two sets of cross section measurements makes it difficult to recommend cross section values for the $\sigma_{\text{sc,t}}(\varepsilon)$ of *c*-C₄F₈. However, we obtained suggested values for $\sigma_{\text{sc,t}}(\varepsilon)$ between 1.1 and 3000 eV by

determining the least squares average of the two sets of measurements in the overlapping energy range of 4–20 eV, and by extending the suggested values to higher and lower energies by normalizing the high energy (≥ 20 eV) cross section data of Nishimura to the average at 20 eV and the low energy (≤ 4 eV) cross section data of Sanabia *et al.* to the average at 4 eV. The resultant suggested cross section $\sigma_{\text{sc,t}}(\varepsilon)$ is shown

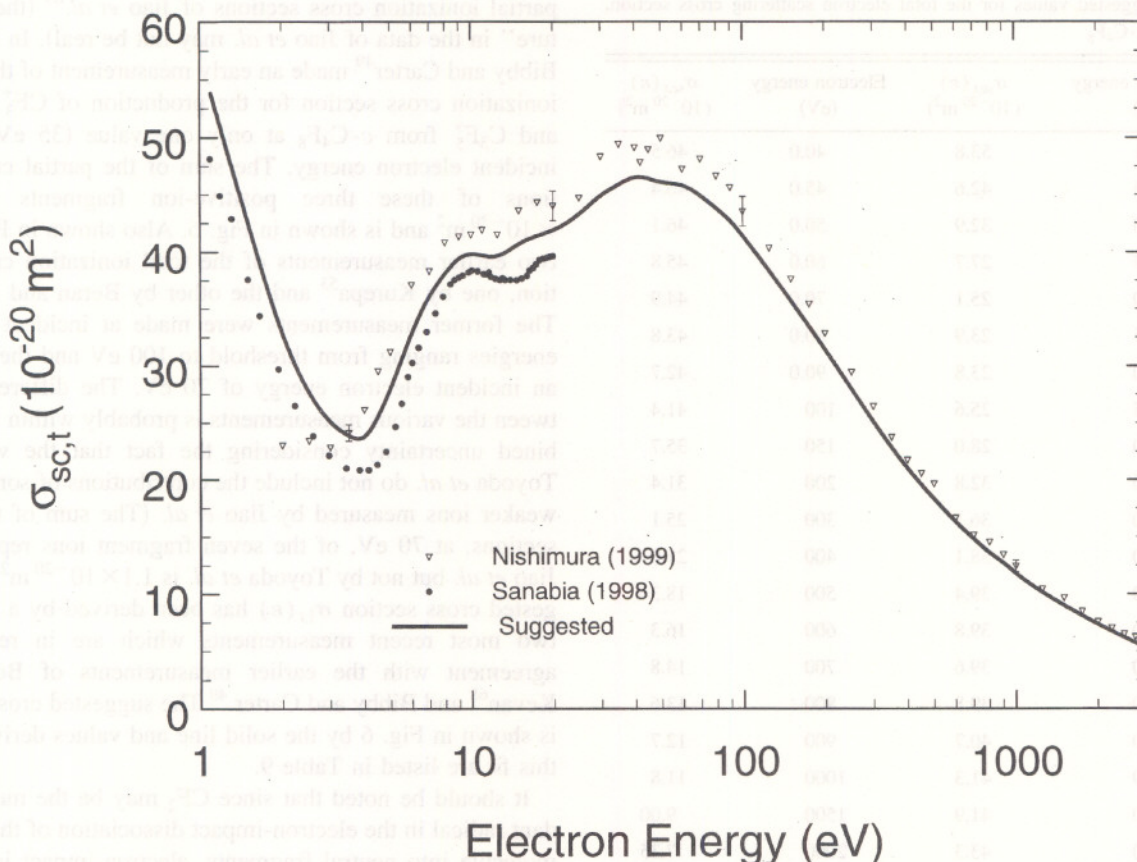


FIG. 2. Total electron scattering cross section, $\sigma_{sc,t}(\epsilon)$, of *c*-C₄F₈: (●) Ref. 57; (▽) Refs. 58, 59; (—) suggested (see text).

in Fig. 2 by the solid line, and values obtained from this line are listed in Table 4.

3.2. Differential elastic electron scattering cross sections, $\sigma_{e,diff}$

Figure 3 shows the recent measurements of $\sigma_{e,diff}$ of *c*-C₄F₈ by Okamoto and co-workers^{60,61} and the calculated values of $\sigma_{e,diff}$ by McKoy and co-workers.⁶² The agreement between the calculated and the measured values of $\sigma_{e,diff}$ is improved as the electron energy is increased. The $\sigma_{e,diff}$ functions show pronounced variations with scattering angle at all electron energies (1.5–100 eV) employed in these investigations. The experimental data for $\sigma_{e,diff}$ are listed in Table 5.

Values of the integral elastic electron scattering cross section $\sigma_{e,int}(\epsilon)$ and the momentum transfer cross section $\sigma_m(\epsilon)$ may be calculated by extrapolating the $\sigma_{e,diff}$ data to 0° and 180° and integrating the curve over all angles. However, these extrapolations and calculations have not been performed in the literature.

3.3. Differential vibrational excitation cross section, $\sigma_{vib,diff}(\epsilon)$

Figure 4 shows the recent measurements of Tanaka and co-workers⁶¹ of the vibrational differential excitation cross

section for an energy loss $\Delta\epsilon=0.15$ eV and a scattering angle θ of 50°. The major peak near 7.5 eV, the rise of the cross section below 3 eV, and the cross section enhancements at ~4.9 and ~11 eV are attributable to the existence of negative ion states at these energies in agreement with the electron attachment and other electron scattering data listed in Table 3. The data in Fig. 4 show the significance of indirect vibrational excitation of the *c*-C₄F₈ molecule by electron impact.

4. Electron Impact Ionization

4.1. Partial ionization cross sections, $\sigma_{i,partial}(\epsilon)$

There have been two measurements of the partial ionization cross sections $\sigma_{i,partial}(\epsilon)$ of *c*-C₄F₈, the first by Toyoda *et al.*⁶³ and the second by Jiao *et al.*^{64,65} Toyoda *et al.*⁶³ used quadrupole mass spectrometry and measured the cross sections for dissociative ionization of the *c*-C₄F₈ molecule by electron impact leading to the formation of CF₂⁺, CF₃⁺, C₂F₃⁺, C₂F₄⁺, and C₃F₅⁺ from threshold to 117.8 eV. Their cross section measurements have an uncertainty of about ±10% and are presented in Table 6 and Fig. 5. Jiao *et al.*^{64,65} measured the $\sigma_{i,partial}(\epsilon)$ of *c*-C₄F₈ from 16 to 200 eV using Fourier transform mass spectrometry. They detected 13 fragment positive ions (see Fig. 5 and Table 7) as opposed to the six reported by Toyoda *et al.* The absolute

TABLE 4. Suggested values for the total electron scattering cross section, $\sigma_{sc,t}(\epsilon)$, of $c\text{-C}_4\text{F}_8$

Electron energy (eV)	$\sigma_{sc,t}(\epsilon)$ (10^{-20} m^2)	Electron energy (eV)	$\sigma_{sc,t}(\epsilon)$ (10^{-20} m^2)
1.1	53.8	40.0	46.5
1.5	42.6	45.0	46.4
2.0	32.9	50.0	46.1
2.5	27.7	60.0	45.8
3.0	25.1	70.0	44.9
3.5	23.9	80.0	43.8
4.0	23.8	90.0	42.7
4.5	25.6	100	41.4
5.0	28.0	150	35.7
6.0	32.8	200	31.4
7.0	36.1	300	25.1
8.0	38.1	400	21.0
9.0	39.4	500	18.3
10.0	39.8	600	16.3
12.0	39.6	700	14.8
13.0	39.8	800	13.6
15.0	40.7	900	12.7
17.0	41.3	1000	11.8
20.0	41.9	1500	9.00
25.0	43.3	2000	7.35
30.0	44.9	2500	6.20
35.0	45.9	3000	5.29

values of their partial ionization cross sections were obtained by normalization to those of Wetzel *et al.*⁶⁶ for argon and have an uncertainty of about $\pm 20\%$. They are listed in Table 7 and are compared in Fig. 5 with those of Toyoda *et al.* and with some early measurements for the production of CF_3^+ , C_2F_4^+ , and C_3F_5^+ at 35 eV by Bibby and Carter.⁴⁹

There are substantial differences between the two sets of measurements which depend on the particular positive ion fragment involved. The parent positive ion $c\text{-C}_4\text{F}_8^+$ was not detected in either of these electron-impact studies^{63,64} or in the photon-impact study of Jarvis *et al.*,⁴⁶ indicating that the ground state of the $c\text{-C}_4\text{F}_8^+$ ion is not bound in the Franck-Condon region. Nevertheless, Smith and Kevan⁶⁷ reported observation of a weak $c\text{-C}_4\text{F}_8^+$ signal in studies of the total and dissociative charge-transfer cross sections of Xe^+ with $c\text{-C}_4\text{F}_8$. These latter observations may indicate a minimum in the potential energy surface of $c\text{-C}_4\text{F}_8^+$ at large internuclear separation distances.

In Table 8 are listed the energy thresholds for the appearance of a number of positive ions by electron (and photon) impact on $c\text{-C}_4\text{F}_8$.

4.2. Total ionization cross section, $\sigma_{i,t}(\epsilon)$

In Fig. 6 is plotted the sum of the partial ionization cross sections of Toyoda *et al.*⁶³ and, similarly, the sum of the

partial ionization cross sections of Jiao *et al.*⁶⁵ (the "structure" in the data of Jiao *et al.* may not be real). In addition, Bibby and Carter⁴⁹ made an early measurement of the partial ionization cross section for the production of CF_3^+ , C_2F_4^+ , and C_3F_5^+ from $c\text{-C}_4\text{F}_8$ at only one value (35 eV) of the incident electron energy. The sum of the partial cross sections of these three positive-ion fragments is $5.35 \times 10^{-20} \text{ m}^2$ and is shown in Fig. 6. Also shown in Fig. 6 are two earlier measurements of the total ionization cross section, one by Kurepa⁵³ and the other by Beran and Kevan.⁶⁸ The former measurements were made at incident electron energies ranging from threshold to 100 eV and the latter at an incident electron energy of 70 eV. The differences between the various measurements is probably within the combined uncertainty considering the fact that the values of Toyoda *et al.* do not include the contributions of some of the weaker ions measured by Jiao *et al.* (The sum of the cross sections, at 70 eV, of the seven fragment ions reported by Jiao *et al.* but not by Toyoda *et al.* is $1.1 \times 10^{-20} \text{ m}^2$). A suggested cross section $\sigma_{i,t}(\epsilon)$ has been derived by a fit to the two most recent measurements which are in reasonable agreement with the earlier measurements of Beran and Kevan⁶⁸ and Bibby and Carter.⁴⁹ The suggested cross section is shown in Fig. 6 by the solid line and values derived from this fit are listed in Table 9.

It should be noted that since CF_2 may be the most abundant radical in the electron-impact dissociation of the $c\text{-C}_4\text{F}_8$ molecule into neutral fragments, electron-impact ionization of this radical may also be important in $c\text{-C}_4\text{F}_8$ plasmas. The electron-impact ionization cross section of the CF_2 radical has been measured by Tarnovsky and Becker⁶⁹ (see also Ref. 22).

4.3. Density-reduced ionization coefficient, $\alpha/N(E/N)$

There have been two experimental determinations of the density-reduced ionization coefficient $\alpha/N(E/N)$ of this molecule by Naidu *et al.*,⁷⁰ over the E/N range from $\sim 300 \times 10^{-17}$ to $\sim 650 \times 10^{-17} \text{ V cm}^2$, and by Tagashira *et al.*⁷¹ for three values of E/N (394×10^{-17} , 425×10^{-17} , and $455 \times 10^{-17} \text{ V cm}^2$). The measurements of Naidu *et al.* were conducted at a gas temperature of 293 K and at two values of the gas pressure, namely 0.084 and 0.1333 kPa. No pressure dependence was observed in their measurements of this quantity. According to Naidu *et al.*, the uncertainty of their data is about $\pm 10\%$ at values of E/N below $(E/N)_{\text{lim}}$ and about $\pm 20\%$ at higher E/N values [$(E/N)_{\text{lim}}$ is the value of (E/N) for which $\alpha = \eta$, where η is the attachment coefficient (Sec. 6)]. These data are plotted in Fig. 7. The solid line is a least squares fit to the data, and values obtained from the fit are listed in Table 10. These values should be treated with caution until they are validated by additional measurements. If these data are used in conjunction with the density-reduced electron attachment coefficient, $\eta/N(E/N)$, of Naidu *et al.*⁷⁰ to determine the density-reduced effective ionization coefficient,

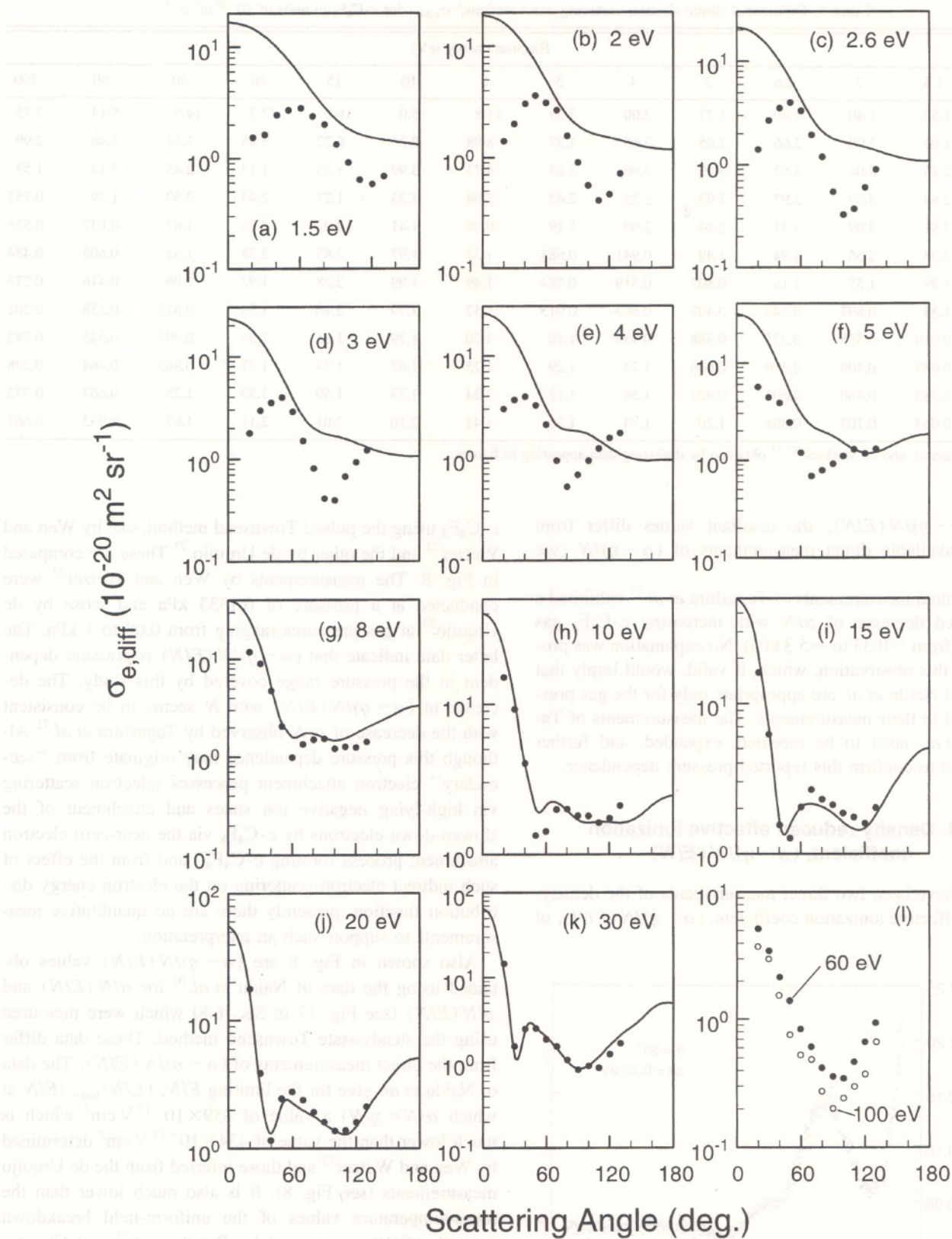


FIG. 3. Differential elastic electron scattering cross sections, $\sigma_{e,diff}$, for *c*-C₄F₈: (●, ○) data of Tanaka and co-workers^{60, 61}; (—) calculations of McKoy *et al.*⁶²

TABLE 5. Differential elastic electron scattering cross sections,^a $\sigma_{e,\text{diff}}$, for $c\text{-C}_4\text{F}_8$ in units of $10^{-20} \text{ m}^2 \text{ sr}^{-1}$

Angle	Electron energy (eV)												
	1.5	2	2.6	3	4	5	8	10	15	20	30	60	100
20°	1.52	1.40	1.40	1.77	3.00	5.59	11.8	15.0	16.0	17.7	14.5	5.14	3.75
30°	1.62	1.99	2.66	2.95	3.66	4.37	8.98	9.20	6.22	3.85	1.54	3.46	2.99
40°	2.43	3.04	3.52	3.49	3.96	3.83	4.73	3.99	1.55	1.15	2.45	2.14	1.53
50°	2.68	3.59	3.97	3.93	3.25	2.42	2.04	1.33	1.27	2.44	2.50	1.39	0.755
60°	2.81	3.09	3.31	2.84	2.09	1.19	0.98	1.41	2.02	2.76	1.87	0.837	0.526
70°	2.38	2.65	1.94	1.49	0.941	0.683	1.33	1.97	2.65	2.38	1.53	0.608	0.484
80°	1.99	1.55	1.18	0.803	0.519	0.784	1.49	1.99	2.28	1.92	1.06	0.416	0.273
90°	1.33	0.897	0.543	0.407	0.683	0.913	1.52	1.79	2.10	1.59	0.813	0.358	0.201
100°	0.910	0.555	0.325	0.388	0.936	1.10	1.20	1.79	1.85	1.36	0.907	0.345	0.242
110°	0.633	0.406	0.370	0.666	1.23	1.29	1.25	1.62	1.74	1.37	0.862	0.464	0.298
120°	0.583	0.460	0.601	0.923	1.56	1.17	1.24	1.73	1.59	1.59	1.25	0.667	0.372
130°	0.683	0.707	0.898	1.20	1.74	1.30	1.41	2.10	2.01	2.11	1.67	0.933	0.667

^aData of Okamoto and co-workers,^{60, 61} obtained by digitizing data appearing in figures.

cient, $(\alpha - \eta)/N(E/N)$, the resultant values differ from the two available direct measurements of $(\alpha - \eta)/N$ (see Fig. 8).

The limited measurements of Tagashira *et al.*⁷¹ exhibited a pronounced decrease of α/N with increasing $c\text{-C}_4\text{F}_8$ gas pressure (from ~ 0.33 to ~ 5.3 kPa). No explanation was provided for this observation, which, if valid, would imply that the data of Naidu *et al.* are appropriate only for the gas pressures used in their measurements. The measurements of Tagashira *et al.* need to be repeated, expanded, and further scrutinized to confirm this reported pressure dependence.

4.4. Density-reduced effective ionization coefficient, $(\alpha - \eta)/N(E/N)$

There have been two direct measurements of the density-reduced effective ionization coefficient, $(\alpha - \eta)/N(E/N)$, of

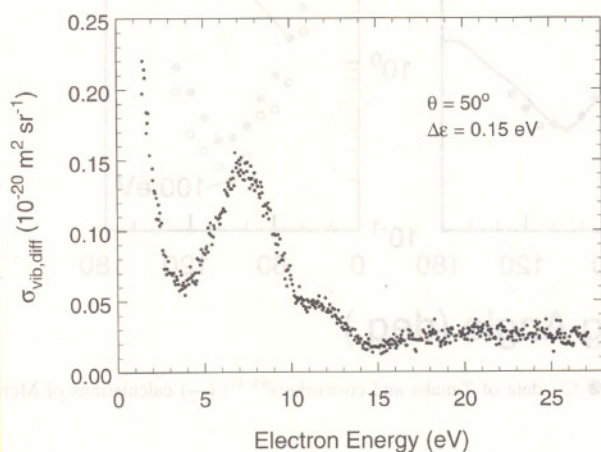


FIG. 4. Vibrational differential electron scattering cross section, $\sigma_{\text{vib,diff}}(\epsilon)$, for $c\text{-C}_4\text{F}_8$ (data of Tanaka *et al.*⁶¹).

$c\text{-C}_4\text{F}_8$ using the pulsed Townsend method, one by Wen and Wetzer⁷² and the other by de Urquijo.⁷³ These are compared in Fig. 8. The measurements by Wen and Wetzer⁷² were conducted at a pressure of 0.1333 kPa and those by de Urquijo⁷³ at gas pressures ranging from 0.08 to 1 kPa. The latter data indicate that $(\alpha - \eta)/N(E/N)$ is pressure dependent in the pressure range covered by this study. The decrease in $(\alpha - \eta)/N(E/N)$ with N seems to be consistent with the decrease of α/N observed by Tagashira *et al.*⁷¹ Although this pressure dependence may originate from "secondary" electron attachment processes (electron scattering via high-lying negative ion states and attachment of the slowed-down electrons by $c\text{-C}_4\text{F}_8$ via the near-zero electron attachment process forming $c\text{-C}_4\text{F}_8^-$) and from the effect of such indirect electron scattering on the electron energy distribution function, presently there are no quantitative measurements to support such an interpretation.

Also shown in Fig. 8 are $(\alpha - \eta)/N(E/N)$ values obtained using the data of Naidu *et al.*⁷⁰ for $\alpha/N(E/N)$ and $\eta/N(E/N)$ (see Fig. 17 in Sec. 6.8) which were measured using the steady-state Townsend method. These data differ from the direct measurements of $(\alpha - \eta)/N(E/N)$. The data of Naidu *et al.* give for the limiting E/N , $(E/N)_{\text{lim}}$, (E/N at which $\alpha/N = \eta/N$) a value of $359 \times 10^{-17} \text{ V cm}^2$ which is much lower than the value of $434 \times 10^{-17} \text{ V cm}^2$ determined by Wen and Wetzer⁷² and those inferred from the de Urquijo measurements (see Fig. 8). It is also much lower than the room-temperature values of the uniform-field breakdown strength $(E/N)_{\text{Br}}$ measured by Berril *et al.*⁷⁴ and Christophorou *et al.*⁷⁵ for this gas. The Berril *et al.* measurements of $(E/N)_{\text{Br}}$ ranged from 428×10^{-17} to $432 \times 10^{-17} \text{ V cm}^2$ and were made at pressures between 10.1 and 60.6 kPa. The value of $(E/N)_{\text{Br}}$ measured by Christophorou *et al.*⁷⁵ is $438 \times 10^{-17} \text{ V cm}^2$ and was made at 69.3 kPa. These compari-

TABLE 6. Partial ionization cross sections,^a $\sigma_{i,\text{partial}}(\varepsilon)$, for *c*-C₄F₈

Electron energy (eV)	$\sigma_{i,\text{partial}}(\varepsilon)$ (10^{-20} m ²)					Sum	
	CF ⁺	CF ₂ ⁺	CF ₃ ⁺	C ₂ F ₃ ⁺	C ₂ F ₄ ⁺		C ₃ F ₅ ⁺
12.8					0.0072	0.0032	0.010
14.8			0.0004				
15.3			0.0007		0.0871	0.0254	0.113
17.8	0.0043	0.0001	0.0115		0.297	0.093	0.406
20.3	0.0342	0.0032	0.0819	0.0001	0.608	0.250	0.977
22.8	0.102	0.0189	0.265	0.0013	0.917	0.439	1.74
25.3	0.215	0.0516	0.573	0.0060	1.17	0.621	2.64
27.8	0.532	0.0984	0.903	0.0137	1.42	0.814	3.78
30.3	0.765	0.146	1.19	0.0262	1.66	1.00	4.79
32.8	1.09	0.195	1.44	0.0362	1.93	1.17	5.86
35.5	1.33	0.245	1.63	0.0440	2.12	1.31	6.68
37.3	1.67	0.303	1.78	0.0513	2.32	1.46	7.58
40.3	1.93	0.341	1.92	0.0557			8.25
42.8	2.21	0.382	2.06	0.0590	2.54	1.69	8.94
45.3	2.42	0.413		0.0631			9.41
47.8	2.67	0.444	2.16	0.0668	2.72	1.85	9.91
50.3	2.81	0.470					10.3
52.8	2.99	0.490	2.28	0.0690	2.93	1.93	10.7
57.8	3.14	0.515	2.30	0.0711	3.00	2.07	11.1
62.8	3.24	0.545	2.35	0.0715	3.11	2.16	11.5
67.8	3.32	0.551	2.39	0.0712	3.15	2.23	11.7
72.8	3.33	0.555	2.45	0.0705	3.12	2.25	11.8
77.8	3.36	0.571	2.47	0.0705	3.17	2.29	11.9
82.8	3.40	0.573	2.48	0.0695	3.18	2.32	12.0
87.8	3.43	0.573	2.48	0.0691	3.17	2.36	12.1
92.8	3.42	0.577	2.48	0.0684	3.16	2.38	12.1
97.8	3.44	0.580	2.46	0.0682	3.17	2.41	12.1
107.8	3.49	0.582	2.43	0.0673	3.16	2.43	12.2
117.8	3.52	0.579	2.41	0.0672	3.21	2.46	12.2

^aData of Toyoda *et al.*⁶³

sons would indicate that the measurements of Naidu *et al.*⁷⁰ for both $\alpha/N(E/N)$ and $\eta/N(E/N)$ require validation by independent measurements.

5. Dissociation into Neutral Fragments

Toyoda *et al.*⁶³ used appearance mass spectrometry in a dual electron beam system to measure the absolute cross sections, $\sigma_{\text{dis,partial}}(\varepsilon)$, for electron-impact dissociation of *c*-C₄F₈ into the neutral radicals CF, CF₂, and CF₃ from threshold to 250 eV. These cross sections, along with their sum, are shown in Fig. 9 and are listed in Table 11. The sum of these partial dissociation cross sections must be taken as a lower limit of the total cross section $\sigma_{\text{dis,neu,t}}(\varepsilon)$ for dissociation of *c*-C₄F₈ into neutrals by electron impact, because other neutral fragments for which the cross sections have not

been measured will contribute to $\sigma_{\text{dis,neu,t}}(\varepsilon)$. For instance, Toyoda *et al.*⁶³ observed C₃F₅ radicals, but reported only the relative cross section for their formation. The stated absolute and relative uncertainties of the cross sections $\sigma_{\text{dis,partial}}(\varepsilon)$ are, respectively, $\pm 100\%$ and $\pm 20\%$.⁶³ However, similar cross sections obtained by the same group for other molecules, such as CF₄ and CHF₃, have been shown to be significantly smaller than their true values.²⁸ The threshold energies for the production of the neutral fragments CF, CF₂, and CF₃ by electron impact on *c*-C₄F₈ as determined by Toyoda *et al.* are, respectively, 14.5, 10.5, and 12.8 eV.

A model calculation predicting radical composition in *c*-C₄F₈ plasmas was conducted by Kazumi *et al.*⁷⁶ This calculation predicts the production of a number of other radicals besides those detected in the measurements of Toyoda *et al.*⁶³

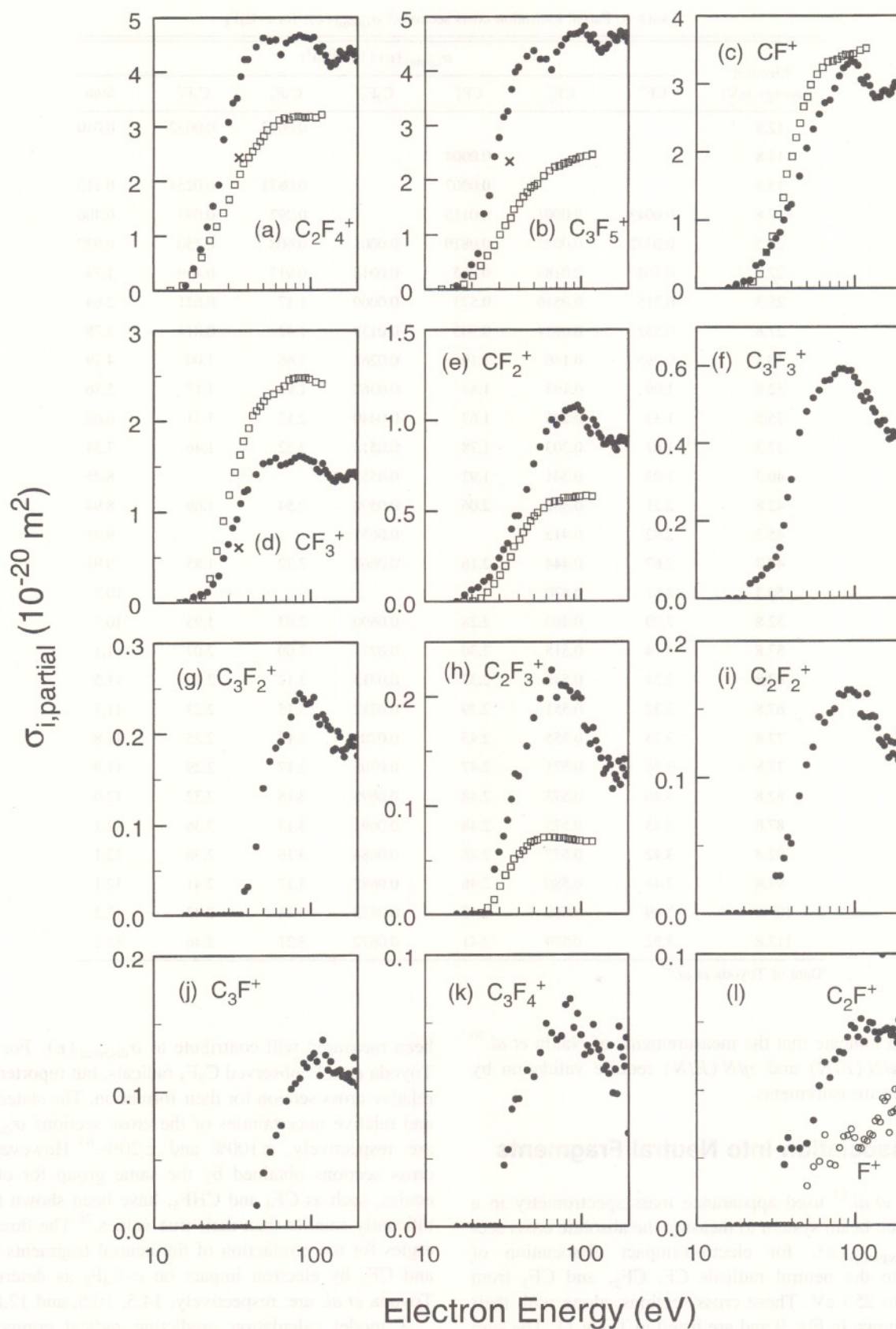


FIG. 5. Partial ionization cross sections, $\sigma_{i,\text{partial}}(\varepsilon)$, of c -C₄F₈: (□) data of Toyoda *et al.*⁶³; (●,○) data of Jiao *et al.*⁶⁵ (×) data of Bibby and Carter.⁴⁹

TABLE 7. Partial ionization cross sections, $\sigma_{i,\text{partial}}(\epsilon)$, for *c*-C₄F₈^a

Electron energy (eV)	$\sigma_{i,\text{partial}}(\epsilon)$ (10 ⁻²⁰ m ²)													Sum
	F ⁺	CF ⁺	C ₂ F ⁺	CF ₂ ⁺	C ₃ F ⁺	C ₂ F ₂ ⁺	CF ₃ ⁺	C ₃ F ₂ ⁺	C ₂ F ₃ ⁺	C ₃ F ₃ ⁺	C ₂ F ₄ ⁺	C ₃ F ₄ ⁺	C ₃ F ₅ ⁺	
16		0.008					0.010				0.087		0.065	0.170
18		0.056		0.036			0.063				0.405		0.263	0.823
20		0.103		0.064			0.090				0.749		0.449	1.46
22		0.117		0.076			0.115			0.038	1.16		0.655	2.16
24		0.334		0.112			0.202			0.048	1.54		1.38	3.62
26		0.374		0.135			0.292			0.059	1.92		1.71	4.48
28		0.531		0.190			0.487		0.041	0.077	2.75		2.42	6.49
30		0.625		0.240			0.641		0.058	0.085	3.07		2.77	7.49
32		0.736		0.285		0.028	0.824		0.072	0.106	3.43	0.023	3.15	8.65
34		0.817	0.028	0.321		0.028	0.918		0.087	0.130	3.51	0.028	3.26	9.14
36		0.997	0.023	0.398		0.041	1.09		0.106	0.187	3.91	0.043	3.66	10.5
38		1.18	0.033	0.473		0.056	1.22	0.027	0.129	0.260	4.22	0.047	3.97	11.6
40		1.23	0.029	0.473		0.052	1.24	0.031	0.127	0.305	4.22	0.047	4.06	11.8
45		1.64	0.029	0.616	0.016	0.086	1.41	0.076	0.154	0.425	4.45	0.058	4.26	13.2
50	0.015	2.05	0.030	0.758	0.040	0.109	1.53	0.140	0.180	0.480	4.62	0.055	4.36	14.4
55	0.022	2.33	0.039	0.850	0.055	0.122	1.55	0.169	0.198	0.516	4.56	0.064	4.21	14.7
60	0.024	2.55	0.052	0.936	0.068	0.144	1.59	0.184	0.214	0.535	4.59	0.075	4.21	15.2
65	0.034	2.72	0.060	0.998	0.075	0.140	1.51	0.191	0.224	0.560	4.31	0.071	4.01	14.9
70	0.023	2.76	0.055	0.970	0.093	0.147	1.53	0.198	0.199	0.563	4.53	0.069	4.34	15.5
75	0.022	2.93	0.061	1.01	0.102	0.150	1.55	0.218	0.210	0.578	4.59	0.070	4.46	15.9
80	0.029	3.11	0.064	1.05	0.106	0.161	1.59	0.236	0.209	0.591	4.64	0.082	4.58	16.4
85	0.033	3.23	0.064	1.06	0.110	0.160	1.61	0.244	0.205	0.591	4.67	0.084	4.67	16.7
90	0.033	3.28	0.069	1.07	0.121	0.164	1.60	0.238	0.199	0.587	4.64	0.073	4.67	16.7
95	0.036	3.33	0.074	1.08	0.118	0.164	1.58	0.232	0.202	0.588	4.62	0.078	4.68	16.8
100	0.032	3.31	0.073	1.05	0.125	0.162	1.56	0.234	0.198	0.569	4.60	0.071	4.72	16.7
105	0.029	3.26	0.070	1.01	0.128	0.160	1.55	0.240	0.172	0.554	4.63	0.063	4.82	16.7
110	0.029	3.06	0.076	0.955	0.122	0.146	1.47	0.218	0.169	0.519	4.44	0.067	4.65	15.9
115	0.032	3.00	0.068	0.924	0.112	0.144	1.44	0.210	0.156	0.508	4.36	0.064	4.56	15.6
120	0.031	3.10	0.072	1.00	0.138	0.161	1.53	0.221	0.171	0.531	4.46	0.074	4.66	16.2
125	0.034	2.97	0.075	0.969	0.127	0.144	1.46	0.215	0.159	0.513	4.29	0.067	4.50	15.5
130	0.033	2.85	0.075	0.922	0.116	0.145	1.41	0.208	0.151	0.488	4.17	0.065	4.38	15.0
135	0.039	2.79	0.071	0.900	0.122	0.144	1.37	0.204	0.143	0.478	4.09	0.062	4.33	14.7
140	0.040	2.80	0.069	0.865	0.114	0.136	1.34	0.181	0.129	0.452	4.16	0.058	4.41	14.8
145	0.038	2.80	0.071	0.864	0.114	0.127	1.33	0.183	0.133	0.446	4.13	0.059	4.40	14.7
150	0.047	2.88	0.100	0.889	0.115	0.125	1.38	0.202	0.143	0.456	4.21	0.056	4.47	15.1
155	0.046	2.90	0.072	0.898	0.116	0.123	1.39	0.196	0.137	0.456	4.36	0.067	4.67	15.4
160	0.047	2.88	0.073	0.872	0.111	0.129	1.37	0.181	0.115	0.430	4.32	0.049	4.64	15.2
165	0.034	2.84	0.072	0.843	0.112	0.114	1.35	0.174	0.128	0.409	4.27	0.058	4.57	15.0
170	0.042	2.86	0.070	0.832	0.110	0.126	1.35	0.183	0.124	0.411	4.23	0.049	4.55	14.9
175	0.042	2.94	0.072	0.880	0.113	0.117	1.40	0.186	0.140	0.427	4.33	0.074	4.64	15.4
180	0.050	3.01	0.070	0.900	0.108	0.125	1.43	0.191	0.119	0.417	4.42	0.066	4.72	15.6
185	0.043	3.01	0.067	0.899	0.107	0.116	1.41	0.196	0.134	0.423	4.37	0.062	4.65	15.5
190	0.050	3.03	0.077	0.881	0.125	0.112	1.43	0.186	0.142	0.424	4.31	0.059	4.62	15.4
195	0.055	3.06	0.073	0.895	0.115	0.132	1.43	0.195	0.127	0.428	4.36	0.070	4.69	15.6
200	0.050	2.97	0.075	0.865	0.104	0.125	1.38	0.175	0.129	0.407	4.18	0.034	4.52	15.0

^aData of Jiao *et al.*⁶⁵

6. Electron Attachment

6.1. Electron beam determined total electron attachment cross section $\sigma_{a,t}(\epsilon)$

A number of electron beam studies^{47,51-54} have shown that at electron energies below ~ 1 eV, the parent negative ion *c*-C₄F₈⁻ is produced. The *c*-C₄F₈^{-*} initially formed by electron capture is unstable with respect to autodetachment.⁷⁷ Under single-collision conditions (low gas pressure) the lifetime of the isolated *c*-C₄F₈^{-*} ion toward autodetachment was found to be between 10 and 15 μ s when measured using time-of-flight mass spectrometry,^{51,54,78} and longer than

~ 200 μ s when measured using ion-cyclotron resonance (ICR) techniques^{79,80} (see Table 12). In the latter case the electrons normally have lower energies than in the former and this may explain the longer lifetime of *c*-C₄F₈^{-*} in the ICR measurements. For a number of other long-lived metastable molecular negative ions it has been found that their autodetachment lifetime decreases as the energy of the attached electron increases (e.g., see Refs. 77 and 81).

Kurepa⁵³ reported a total electron attachment cross section, $\sigma_{a,t}(\epsilon)$, for *c*-C₄F₈ which below ~ 1 eV should represent the cross section for the formation of the parent negative ion *c*-C₄F₈⁻ (see discussion later in this section). This cross

TABLE 8. Energy thresholds for the appearance of positive-ion fragments by electron impact on $c\text{-C}_4\text{F}_8$

Positive ion fragment	Energy threshold (eV)	Reference
C_3F_5^+	11.6 ± 0.2^a	46
	12.1 ± 0.1	47
C_2F_4^+	11.8^a	46
	12.35 ± 0.1	47
CF_3^+	14.4 ± 0.2	47
	18.1	63
CF_2^+	20.3	63
CF^+	18.4 ± 0.2	47
	19.2	63

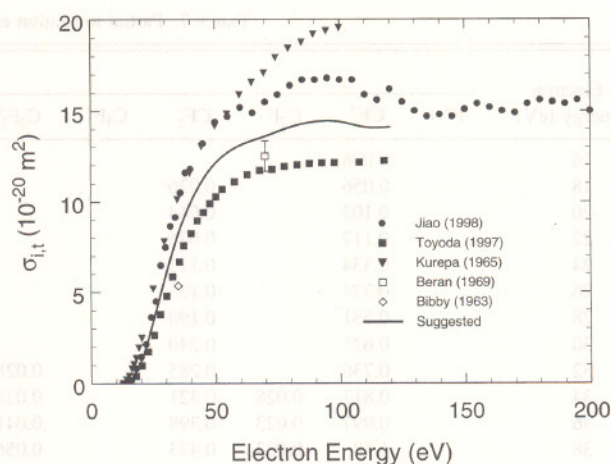
^aPhoton-impact value, the rest of the data listed are electron-impact results.

TABLE 9. Suggested values for the total ionization cross section, $\sigma_{\text{it}}(\varepsilon)$, of $c\text{-C}_4\text{F}_8$

Electron energy (eV)	$\sigma_{\text{it}}(\varepsilon)$ (10^{-20} m^2)	Electron energy (eV)	$\sigma_{\text{it}}(\varepsilon)$ (10^{-20} m^2)
14.0	0.02	40.0	9.92
15.0	0.07	45.0	11.2
16.0	0.21	50.0	12.1
17.0	0.42	60.0	13.1
18.0	0.66	70.0	13.6
19.0	0.89	80.0	14.1
20.0	1.21	90.0	14.4
25.0	3.44	100	14.4
30.0	5.93	110	14.1
35.0	8.18	120	14.1

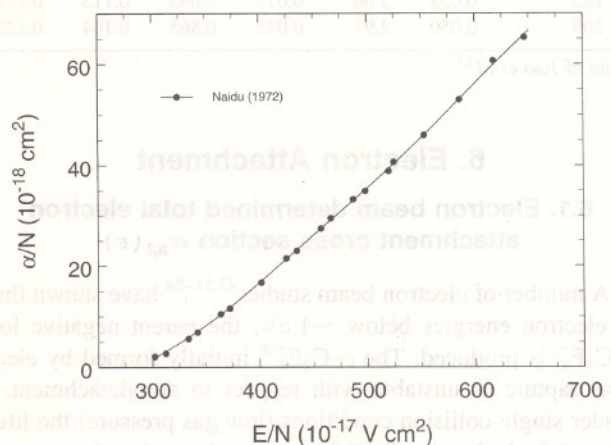
TABLE 10. Values of the density-reduced ionization coefficient, $\alpha/N(E/N)$, for $c\text{-C}_4\text{F}_8$ derived from a fit to the data of Naidu *et al.*⁷⁰

E/N (10^{-17} V cm^2)	$\alpha/N(E/N)$ (10^{-18} cm^2)
300	1.6
350	8.27
400	16.7
450	26.1
500	35.5
550	45.5
600	56.2
650	66.6

FIG. 6. Total ionization cross section, $\sigma_{\text{it}}(\varepsilon)$, of $c\text{-C}_4\text{F}_8$: (●) Ref. 65; (■) Ref. 63; (▼) Ref. 53; (□) Ref. 68; (◇) Ref. 49; (—) suggested.

section is shown in Fig. 10. In plotting these data we assigned the maximum value of the cross section for the formation of $c\text{-C}_4\text{F}_8^-$ at 0.4 eV to be the value of $0.21 \times 10^{-20} \text{ m}^2$ listed by Kurepa in Table 5 of his paper.⁵³ In Fig. 10 is also plotted the low energy, electron-beam-determined cross section for the formation of $c\text{-C}_4\text{F}_8^-$ by Chutjian and Alajajian.⁸² These investigators used their krypton photoionization technique and put their relative measurements on an absolute scale by normalization to the swarm data of Christodoulides *et al.*⁸³ These cross sections are discussed further in Sec. 6.5 where they are compared with the total electron attachment cross sections obtained from electron swarm data.

Prior to presenting and discussing the electron swarm data, we present and discuss here the relative cross section data obtained by electron beam investigations of the production of the various fragment negative ions formed by electron impact on $c\text{-C}_4\text{F}_8$. These studies^{47,49,51,53-55,84} have shown the formation of many fragment negative ions via a number of negative ion states in the electron energy range between ~ 2 and ~ 15 eV. The most systematic measurements of the relative cross sections for the production of the various frag-

FIG. 7. Density-reduced ionization coefficient, $\alpha/N(E/N)$, for $c\text{-C}_4\text{F}_8$ (data of Naidu *et al.*⁷⁰).

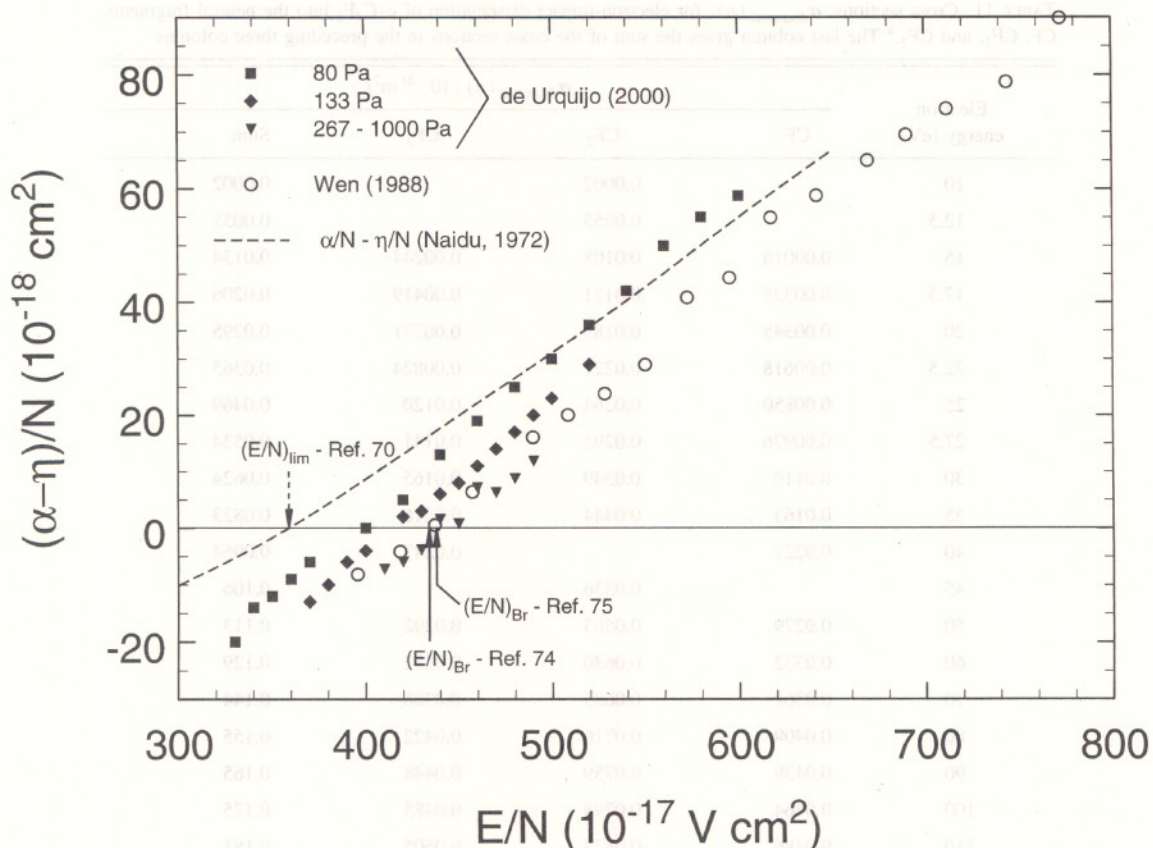


FIG. 8. Density-reduced effective ionization coefficient, $(\alpha - \eta)/N$ (E/N), for *c*-C₄F₈. (○) Ref. 72; (■, ◆, ▼) Ref. 73; (---), $\alpha/N - \eta/N$ Ref. 70; the broken arrow shows the $(E/N)_{\text{lim}}$ value of Ref. 70 and the solid arrows represent the values of $(E/N)_{\text{Br}}$ as measured in Refs. 72, 74 and 75.

ment negative ions as a function of the electron energy in absolute relation to each other were made by Sauer *et al.*⁵¹ using time-of-flight mass spectrometry. These relative cross sections are shown in Fig. 11 along with the relative cross section for the production of the parent negative ion

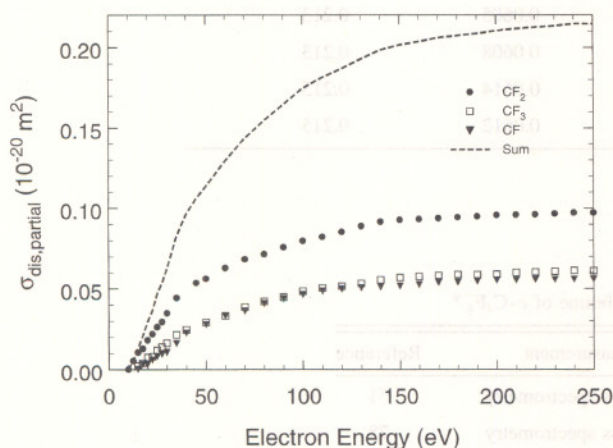


FIG. 9. Partial cross sections, $\sigma_{\text{dis,partial}}(\epsilon)$, for electron-impact dissociation of *c*-C₄F₈ into the neutral fragments CF (▼), CF₂ (●), and CF₃ (□). The data are from Toyoda *et al.*,⁶³ and the broken line (---) represents the sum of the partial cross sections for the three fragments.

c-C₄F₈^{-*} at electron energies below 1.5 eV. The most abundant fragment negative ion is seen to be F⁻. This ion is formed via a number of negative ion states. Recent measurements⁸⁵ of the negative-ion density in a high density *c*-C₄F₈ plasma using a laser photodetachment technique, indicating the major negative ion species to be F⁻, are consistent with these findings.

The other observed negative ion fragments (CF₃⁻, C₂F₃⁻, C₃F₅⁻) have much lower cross sections than F⁻ as they require multiple bond breaking and molecular rearrangement. All four fragment negative ions (F⁻, CF₃⁻, C₂F₃⁻, and C₃F₅⁻) are produced at electron energies between 4 and 5 eV, indicating the existence of a common negative ion state in this energy range. There is general agreement among the electron-beam studies^{47,49,51,53-55,84} as to the positions of the various peaks in the relative yields of the various negative ions (see Table 3) except for the peak at 1.75 eV reported by Lifshitz and Grajower,⁴⁷ which was not observed in any of the other electron-beam studies.

Three of the electron-beam studies^{49,53,55} reported absolute cross sections for some ions at their peak energies. These are summarized in Table 13. They disagree considerably with each other, and with the electron swarm data discussed later (Secs. 6.4 and 6.5) in this paper.

TABLE 11. Cross sections, $\sigma_{\text{dis,partial}}(\epsilon)$, for electron-impact dissociation of $c\text{-C}_4\text{F}_8$ into the neutral fragments CF, CF_2 , and CF_3 .^a The last column gives the sum of the cross sections in the preceding three columns

Electron energy (eV)	$\sigma_{\text{dis,partial}}(\epsilon) (10^{-20} \text{ m}^2)$			Sum
	CF	CF_2	CF_3	
10		0.0002		0.0002
12.5		0.0055		0.0055
15	0.00016	0.0108	0.00244	0.0134
17.5	0.00335	0.0131	0.00419	0.0206
20	0.00345	0.0183	0.00771	0.0295
22.5	0.00618	0.0221	0.00824	0.0365
25	0.00850	0.0264	0.0120	0.0469
27.5	0.00976	0.0295	0.0141	0.0534
30	0.0110	0.0349	0.0165	0.0624
35	0.0163	0.0444	0.0216	0.0823
40	0.0227		0.0247	0.0964
45		0.0536		0.106
50	0.0279	0.0563	0.0292	0.113
60	0.0332	0.0630	0.0332	0.129
70	0.0362	0.0685	0.0388	0.144
80	0.0409	0.0716	0.0422	0.155
90	0.0439	0.0759	0.0448	0.165
100	0.0464	0.0798	0.0485	0.175
110	0.0486	0.0823	0.0505	0.181
120	0.0498	0.0854	0.0516	0.187
130	0.0506	0.0890	0.0533	0.193
140	0.0511	0.0917	0.0556	0.198
150	0.0517	0.0928	0.0570	0.202
160	0.0526	0.0933	0.0577	0.204
170	0.0538	0.0939	0.0583	0.206
180	0.0541	0.0944	0.0588	0.207
190	0.0547	0.0950	0.0588	0.209
200	0.0554	0.0958	0.0591	0.210
210	0.0554	0.0961	0.0601	0.212
220	0.0557	0.0963	0.0605	0.213
230	0.0558	0.0967	0.0608	0.213
240	0.0559	0.0973	0.0614	0.215
250	0.0560	0.0973	0.0612	0.215

^aData of Toyoda *et al.*⁶³

TABLE 12. Autodetachment lifetime of $c\text{-C}_4\text{F}_8^{*}$

Lifetime (s)	Method of measurement	Reference
10×10^{-6}	Time-of-flight mass spectrometry	51
12×10^{-6}	Time-of-flight mass spectrometry	78
14.8×10^{-6}	Time-of-flight mass spectrometry	54
$\sim 200 \times 10^{-6}$	Ion cyclotron resonance	79
500×10^{-6}	Ion cyclotron resonance	80

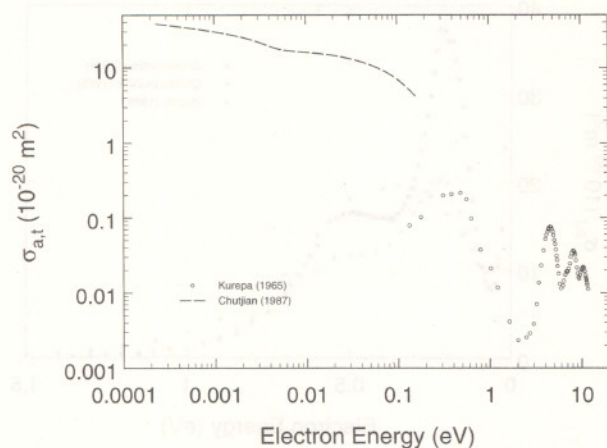


FIG. 10. Total electron attachment cross section, $\sigma_{a,t}(\epsilon)$, as a function of electron energy for *c*-C₄F₈ measured using electron beam techniques: (○) Ref. 53; (---) Ref. 82. The cross section below ~ 1 eV is due to the formation of *c*-C₄F₈⁻.

6.2. Total electron attachment rate constant as a function of E/N , $k_{a,t}(E/N)$

There have been two measurements of the total electron attachment rate constant, $k_{a,t}(E/N)$, as a function of the density-reduced electric field E/N employing electron-swarm techniques and mixtures of *c*-C₄F₈ with the buffer gases of N₂ and Ar.^{83,86} These room temperature ($T = 298$ K) measurements are shown in Fig. 12.

6.3. Total electron attachment rate constant as a function of the mean electron energy, $k_{a,t}(\langle\epsilon\rangle)$

The total electron attachment rate constant, $k_{a,t}(\langle\epsilon\rangle)$, as a function of the mean electron energy $\langle\epsilon\rangle$ can be determined from the swarm measurements of $k_{a,t}(E/N)$ in the buffer gases N₂ and Ar shown in Fig. 12 since the electron energy

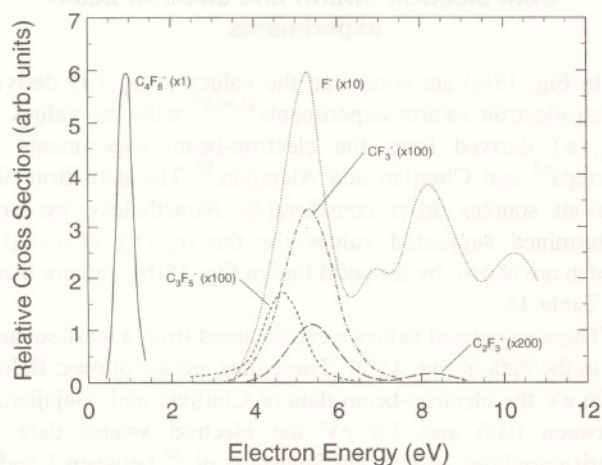


FIG. 11. Relative cross sections for the formation of the parent *c*-C₄F₈⁻ and the fragment F⁻, CF₃⁻, C₂F₃⁻, and C₃F₅⁻ negative ions by electron attachment to *c*-C₄F₈ (note the multiplication factors) by Sauer *et al.*⁵¹

TABLE 13. Peak cross section values for negative ion fragments formed by electron impact on *c*-C₄F₈ (see text)

Peak cross section value (10 ⁻¹⁸ cm ²)	Peak energy (eV)	Fragment ion	Reference
236	4.3	F ⁻	49
0.9	4.95	F ⁻	55
7.56	4.5	total ^a	53
0.2	7.4	F ⁻	55
1.90	6.9	total ^a	53
0.4	8.6	F ⁻	55
3.60	8.1	total ^a	53
0.5	10.8	F ⁻	55
2.25	10.4	total ^a	53
11.1	5.0	CF ₃ ⁻	49
0.001	4.95	CF ₃ ⁻	55

^aAbout equal to that for the production of F⁻ at this energy.

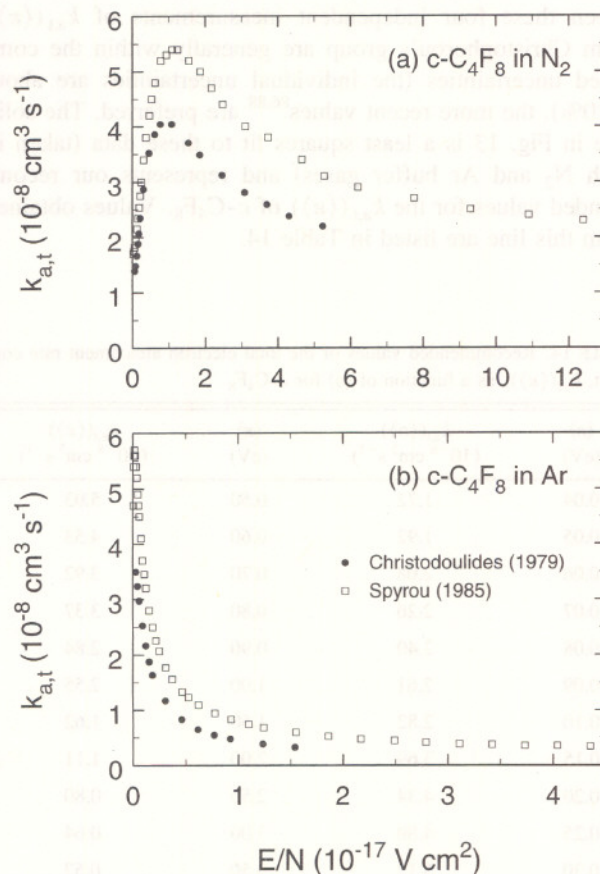


FIG. 12. Total electron attachment rate constant, $k_{a,t}(E/N)$, as a function of E/N for *c*-C₄F₈ measured in the buffer gas (a) N₂ and (b) Ar: (●) Ref. 83; (□) Ref. 86.

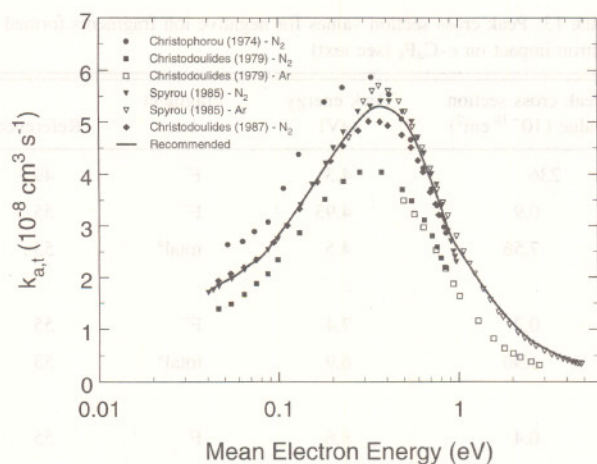


FIG. 13. Total electron attachment rate constant, $k_{a,t}(\langle \epsilon \rangle)$, as a function of $\langle \epsilon \rangle$ for $c\text{-C}_4\text{F}_8$: (●) Ref. 87; (■, □) Ref. 83; (▼, ▽) Ref. 86; (◆) Ref. 88; (—) recommended. Data shown by closed symbols were obtained in N_2 buffer gas, and data shown by open symbols were obtained in Ar buffer gas.

distribution function is known for each value of E/N at which the $k_{a,t}$ was measured in the buffer gases N_2 and Ar. These room-temperature ($T=298\text{ K}$) measurements of $k_{a,t}(\langle \epsilon \rangle)$ are shown in Fig. 13, along with two other measurements of $k_{a,t}(\langle \epsilon \rangle)$.^{87,88} Although the differences between these four independent measurements of $k_{a,t}(\langle \epsilon \rangle)$ from Christophorou's group are generally within the combined uncertainties (the individual uncertainties are about $\pm 10\%$), the more recent values^{86,88} are preferred. The solid line in Fig. 13 is a least squares fit to these data (taken in both N_2 and Ar buffer gases) and represents our recommended values for the $k_{a,t}(\langle \epsilon \rangle)$ of $c\text{-C}_4\text{F}_8$. Values obtained from this line are listed in Table 14.

TABLE 14. Recommended values of the total electron attachment rate constant, $k_{a,t}(\langle \epsilon \rangle)$, as a function of $\langle \epsilon \rangle$ for $c\text{-C}_4\text{F}_8$

$\langle \epsilon \rangle$ (eV)	$k_{a,t}(\langle \epsilon \rangle)$ ($10^{-8}\text{ cm}^3\text{ s}^{-1}$)	$\langle \epsilon \rangle$ (eV)	$k_{a,t}(\langle \epsilon \rangle)$ ($10^{-8}\text{ cm}^3\text{ s}^{-1}$)
0.04	1.72	0.50	5.03
0.05	1.92	0.60	4.53
0.06	2.08	0.70	3.92
0.07	2.26	0.80	3.37
0.08	2.40	0.90	2.84
0.09	2.61	1.00	2.55
0.10	2.82	1.50	1.62
0.15	3.69	2.00	1.11
0.20	4.34	2.50	0.80
0.25	4.80	3.00	0.64
0.30	5.12	3.50	0.52
0.35	5.29	4.00	0.43
0.40	5.28	4.50	0.35

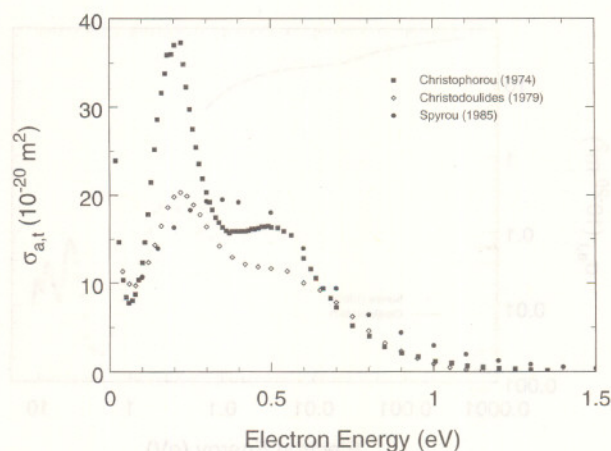


FIG. 14. Swarm-determined total electron attachment cross section, $\sigma_{a,t}(\epsilon)$, as a function of electron energy ($\leq 1.5\text{ eV}$) for $c\text{-C}_4\text{F}_8$: (■) Ref. 87; (◇) Ref. 83; (●) Ref. 86.

6.4. Swarm-unfolded total electron attachment cross section, $\sigma_{a,t}(\epsilon)$

In Fig. 14 are shown the values of the total electron attachment cross section, $\sigma_{a,t}(\epsilon)$, for $c\text{-C}_4\text{F}_8$ at energies below 1.5 eV . These have been obtained by Christophorou and co-workers^{83,86,87} from an unfolding of their $k_{a,t}(E/N)$ data measured in mixtures of $c\text{-C}_4\text{F}_8$ with the buffer gases N_2 ^{83,87} and Ar.⁸⁶ The respective electron energy distribution functions were used for each buffer gas. While the cross section from the most recent measurement exhibits a peak near 0.4 eV , the earlier data of Christophorou *et al.*⁸⁷ indicate a "double peak" with a distinct maximum near 0.2 eV . It may be possible that the peak near 0.2 eV in the earliest data resulted from unfolding errors or from an uncertainty in the electron energy distribution functions of N_2 that were used at the time. For this reason we shall not consider this cross section further.

6.5. Comparison of the values of $\sigma_{a,t}(\epsilon)$ derived from electron swarm and electron beam experiments

In Fig. 15(a) are compared the values of $\sigma_{a,t}(\epsilon)$ derived from electron swarm experiments^{83,86,87} with the values of $\sigma_{a,t}(\epsilon)$ derived from the electron-beam experiments of Kurepa⁵³ and Chutjian and Alajajian.⁸² The data from the various sources differ considerably. Nonetheless, we have determined suggested values for the $\sigma_{a,t}(\epsilon)$ of $c\text{-C}_4\text{F}_8$, which are shown by the solid line in Fig. 15(b), and are listed in Table 15.

These suggested values were obtained from a least-squares fit to the data in Fig. 15(b). These data are as follows: Below 0.06 eV the electron-beam data of Chutjian and Alajajian;⁸² between 0.06 and 1.0 eV the electron swarm data of Christodoulides *et al.*⁸³ and Spyrou *et al.*,⁸⁶ between 1 and 3 eV the data of Spyrou *et al.*⁸⁶ derived from measurements in Ar buffer gas and normalized to the average of the Christodoulides *et al.*⁸³ and Spyrou *et al.*⁸⁶ data at 1 eV ; and

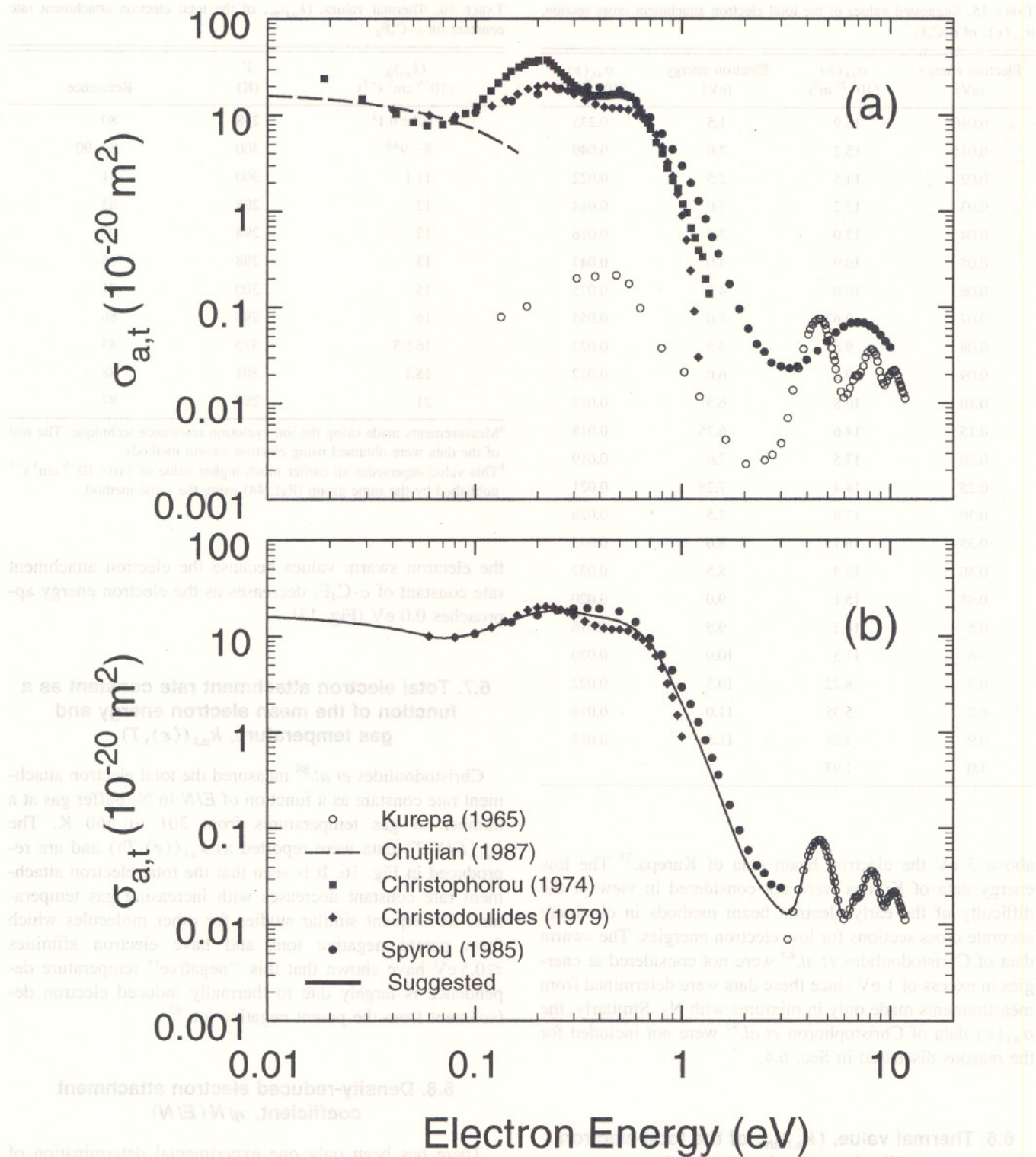


FIG. 15. (a) Comparison of electron swarm and electron beam data for the total electron attachment cross section, $\sigma_{a,t}(\epsilon)$, of *c*-C₄F₈. Electron-swarm data: (■) Ref. 87; (◆) Ref. 83; (●) Ref. 86. Electron-beam data: (○) Ref. 53; (---) Ref. 82. (b) Data of Ref. 82 (---) below 0.06 eV (hidden behind solid line); data of Refs. 83 (◆) and 86 (●) between 0.06 and 3.0 eV; data of Ref. 53 (○) above 3 eV. (—) Suggested.

TABLE 15. Suggested values of the total electron attachment cross section, $\sigma_{a,t}(\varepsilon)$, of $c\text{-C}_4\text{F}_8$

Electron energy (eV)	$\sigma_{a,t}(\varepsilon)$ (10^{-20} m^2)	Electron energy (eV)	$\sigma_{a,t}(\varepsilon)$ (10^{-20} m^2)
0.010	15.9	1.5	0.235
0.015	15.2	2.0	0.049
0.02	14.5	2.5	0.022
0.03	13.2	3.0	0.014
0.04	12.0	3.5	0.016
0.05	10.9	4.0	0.047
0.06	10.0	4.5	0.075
0.07	9.67	5.0	0.055
0.08	9.83	5.5	0.022
0.09	10.2	6.0	0.012
0.10	10.8	6.5	0.015
0.15	14.6	6.75	0.018
0.20	17.5	7.0	0.019
0.25	18.4	7.25	0.021
0.30	17.8	7.5	0.026
0.35	16.7	8.0	0.035
0.40	15.8	8.5	0.032
0.45	15.1	9.0	0.020
0.5	14.2	9.5	0.016
0.6	11.5	10.0	0.020
0.7	8.22	10.5	0.022
0.8	5.35	11.0	0.018
0.9	3.24	11.5	0.013
1.0	1.97		

above 3 eV the electron beam data of Kurepa.⁵³ The low energy data of Kurepa were not considered in view of the difficulty of the early electron beam methods in obtaining accurate cross sections for low electron energies. The swarm data of Christodoulides *et al.*⁸³ were not considered at energies in excess of 1 eV since these data were determined from measurements made only in mixtures with N_2 . Similarly, the $\sigma_{a,t}(\varepsilon)$ data of Christophorou *et al.*⁸⁷ were not included for the reasons discussed in Sec. 6.4.

6.6. Thermal value, $(k_{a,t})_{th}$, of the total electron attachment rate constant

The published experimental data on $(k_{a,t})_{th}$ are listed in Table 16. If the lowest two measurements are excluded, the average of the remaining eight room-temperature measurements is $1.5 \times 10^{-8} \text{ cm}^3 \text{ s}^{-1}$. The lowest two values in Table 16 were measured using the ICR technique in which the electron energies are generally lower than the "thermal" electron energies in the electron swarm experiments. Thus the ICR-measured magnitudes of $(k_{a,t})_{th}$ may be lower than

TABLE 16. Thermal values, $(k_{a,t})_{th}$, of the total electron attachment rate constant for $c\text{-C}_4\text{F}_8$

$(k_{a,t})_{th}$ ($10^{-9} \text{ cm}^3 \text{ s}^{-1}$)	T (K)	Reference
0.4 ± 0.1^a	298	80
$8 - 9^{a,b}$	300	89, 90
11.1	300	91
12	298	83
12	298	92
13	298	16
15	300	21
16	298	86
16 ± 5	375	43
18.1	301	88
21	298	87

^aMeasurements made using the ion cyclotron resonance technique. The rest of the data were obtained using electron swarm methods.

^bThis value supersedes an earlier much higher value of $110 \times 10^{-9} \text{ cm}^3 \text{ s}^{-1}$ published by the same group (Ref. 44) using the same method.

the electron swarm values because the electron attachment rate constant of $c\text{-C}_4\text{F}_8$ decreases as the electron energy approaches 0.0 eV (Fig. 13).

6.7. Total electron attachment rate constant as a function of the mean electron energy and gas temperature, $k_{a,t}(\langle\varepsilon\rangle, T)$

Christodoulides *et al.*⁸⁸ measured the total electron attachment rate constant as a function of E/N in N_2 buffer gas at a number of gas temperatures from 301 to 560 K. The $k_{a,t}(E/N, T)$ data were reported as $k_{a,t}(\langle\varepsilon\rangle, T)$ and are reproduced in Fig. 16. It is seen that the total electron attachment rate constant decreases with increasing gas temperature. Subsequent similar studies for other molecules which form parent negative ions and have electron affinities $\leq 0.5 \text{ eV}$ have shown that this "negative" temperature dependence is largely due to thermally induced electron detachment from the parent negative ion.⁹³

6.8. Density-reduced electron attachment coefficient, $\eta/N(E/N)$

There has been only one experimental determination of the density-reduced electron attachment coefficient, $\eta/N(E/N)$, of $c\text{-C}_4\text{F}_8$ over an extended range of E/N , namely, that by Naidu *et al.*⁷⁰ shown in Fig. 17. These measurements were made at a temperature of 293 K and at two values of the gas pressure (0.084 and 0.133 kPa). They have a quoted uncertainty of about $\pm 10\%$ for E/N values below $(E/N)_{lim}$ and about $\pm 20\%$ for E/N values above $(E/N)_{lim}$. The solid line shown in Fig. 17 is a least squares fit to the data. Values obtained from this fit are listed in Table 17. For

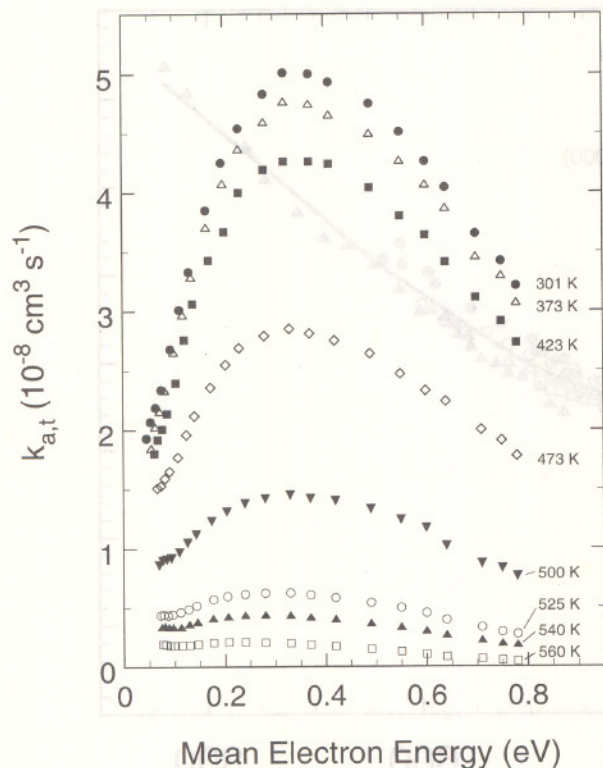


FIG. 16. Total electron attachment rate constant as a function of $\langle \varepsilon \rangle$ and T , $k_{a,t}(\langle \varepsilon \rangle, T)$, for *c*-C₄F₈ (data of Christodoulides *et al.*⁸⁸).

the reasons discussed in Sec. 4.4, and the fact that limited measurements by Tagashira *et al.*⁷¹ indicate a decrease in η/N with gas pressure, these values require further validation.

7. Electron Transport

7.1. Electron drift velocity, $w(E/N)$

In Fig. 18 are shown the measurements of Naidu *et al.*⁷⁰ for the electron drift velocity, $w(E/N)$, in *c*-C₄F₈ made at

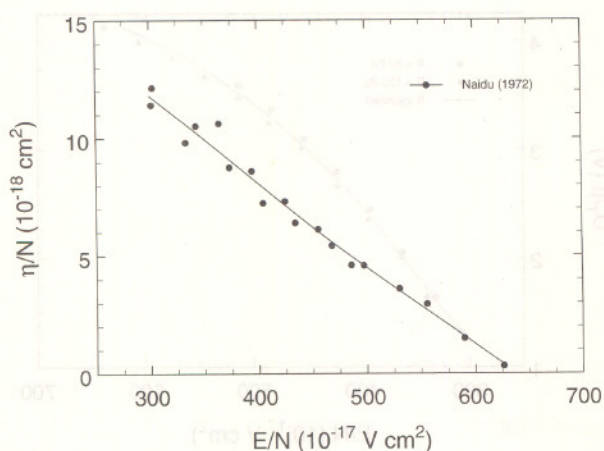


FIG. 17. Density-reduced electron attachment coefficient, $\eta/N(E/N)$, for *c*-C₄F₈ (data of Naidu *et al.*⁷⁰).

TABLE 17. Values of $\eta/N(E/N)$ for *c*-C₄F₈ ($T=293$ K) derived from a fit to the data of Naidu *et al.*⁷⁰

E/N (10^{-17} V cm ²)	$\eta/N(E/N)$ (10^{-18} cm ²)
300	11.8
350	9.98
400	8.10
450	6.22
500	4.49
550	2.87
600	1.25
625	0.43

293 K. The overall uncertainty in these data was quoted by Naidu *et al.* to be less than $\pm 5\%$. Also shown in Fig. 18 are the results of room temperature measurements of $w(E/N)$ by Wen and Wetzer⁷² and by de Urquijo.⁷³ The measurements by de Urquijo were obtained for a number of gas pressures (see figure legend), and seem to indicate a small decrease of the electron drift velocity with increasing gas pressure. The solid line shown in Fig. 18 is a least squares fit to the data of Naidu *et al.*, Wen and Wetzer, and de Urquijo. Values obtained from this line are listed in Table 18 as the presently suggested values for the $w(E/N)$ of *c*-C₄F₈.

Measurements of $w(E/N)$ in two mixtures of *c*-C₄F₈ with Ar at relative concentrations of 0.468% and 4.91% have recently been reported by Yamaji *et al.*⁹⁴ They may be of interest to those using Boltzmann codes for the calculation of electron transport parameters in *c*-C₄F₈.

7.2. Ratio of the lateral electron diffusion coefficient to electron mobility, $D_T/\mu(E/N)$

The $D_T/\mu(E/N)$ measurements by Naidu *et al.*⁷⁰ seem to be the only available data for this gas. They were obtained at 293 K for two gas pressures (0.084 and 0.133 kPa). Their overall uncertainty is quoted by Naidu *et al.* to vary “between about $\pm 5\%$ at the lowest E/N and about $\pm 3\%$ at the high E/N values.” These data are shown in Fig. 19. Although the data indicate a slight pressure dependence of $D_T/\mu(E/N)$, this variation is within the combined uncertainty of the measurements made at the two pressures. Thus, we performed a least squares fit to all the data in Fig. 19, which is shown by the solid line in the figure. Values from this fit are listed in Table 19 as the suggested data for the $D_T/\mu(E/N)$ of *c*-C₄F₈.

For measurements of $D_T/\mu(E/N)$ in two mixtures of *c*-C₄F₈ with Ar at relative concentrations of 0.468% and 4.91% see Yamaji *et al.*⁹⁴

8. Ion–Molecule Reactions

There are three studies of ion–molecule reactions involving *c*-C₄F₈ which might be of interest to its use as a plasma processing gas. The first study is by Smith and Kevan⁶⁷ who

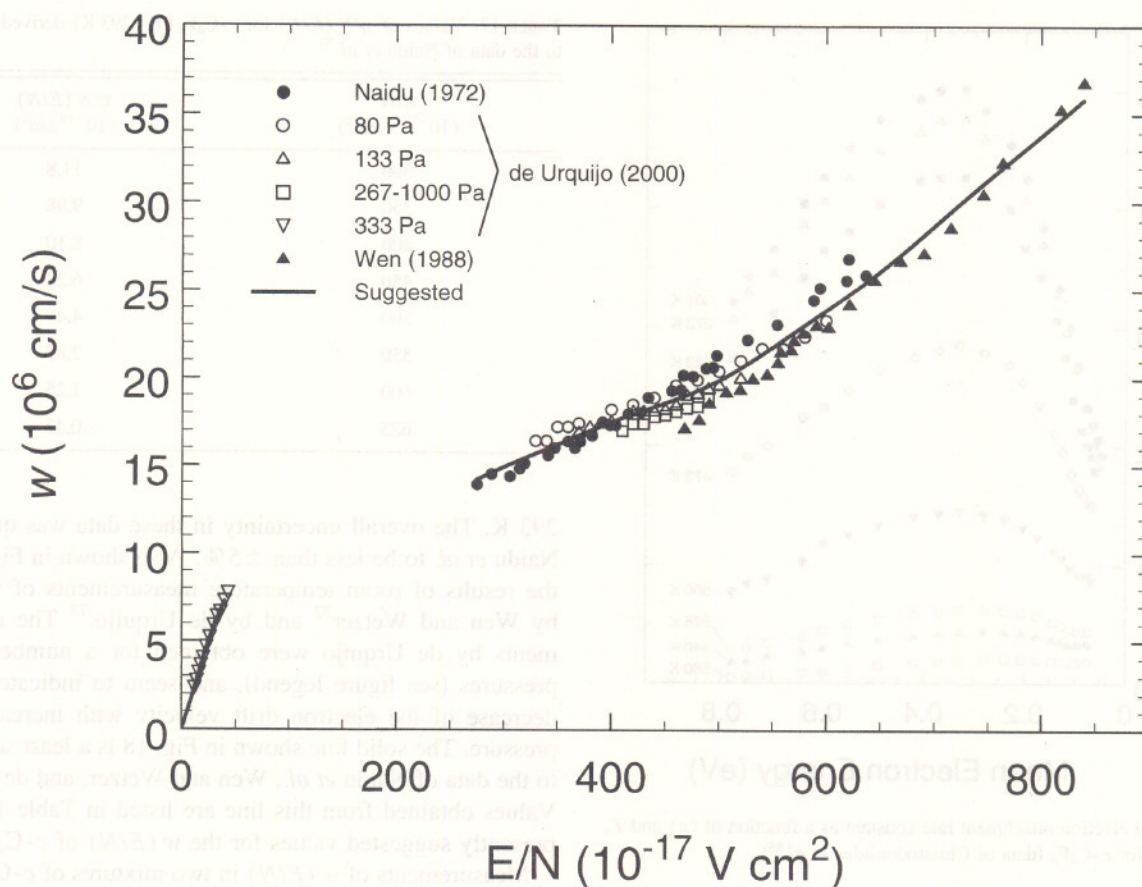


FIG. 18. Electron drift velocity, $w(E/N)$, for $c\text{-C}_4\text{F}_8$ at room temperature: (●) Ref. 70; (○, △, □, ▽) Ref. 73; (▲) Ref. 72; (—) suggested.

measured the cross sections for total and dissociative charge transfer in collisions of rare-gas positive ions with $c\text{-C}_4\text{F}_8$. They found that in such collisions the predominant ion is C_2F_4^+ at recombination energies of up to 16 eV. Only for Xe^+ bombardment did they detect a small parent positive ion $c\text{-C}_4\text{F}_8^+$. The second study is by Su and Kevan⁹⁵ on ion-molecule reactions in $c\text{-C}_4\text{F}_8$ using ICR mass spectrometry.

TABLE 18. Suggested room-temperature values of the electron drift velocity, $w(E/N)$, for $c\text{-C}_4\text{F}_8$

E/N (10^{-17} V cm^2)	$w(E/N)$ (10^6 cm s^{-1})	E/N (10^{-17} V cm^2)	$w(E/N)$ (10^6 cm s^{-1})
0	0.00	450	18.6
10	1.91	500	19.9
20	4.02	550	21.8
30	5.83	600	23.9
40	7.28	650	26.1
—	—	700	28.7
275	14.2	750	31.3
300	14.9	800	33.8
350	16.2	840	35.9
400	17.5		

These studies have shown that fluoride transfer and collision-induced dissociation reactions predominate. The third study is by Morris *et al.*⁹⁶ who measured the rate constants and product branching ratios for reactions of the atmospheric ions O^+ , O_2^+ , O^- , O_2^- , NO^+ , H_3O^+ , CO_3^- , and NO_3^- with $c\text{-C}_4\text{F}_8$. They found that the last four ions are unreactive.

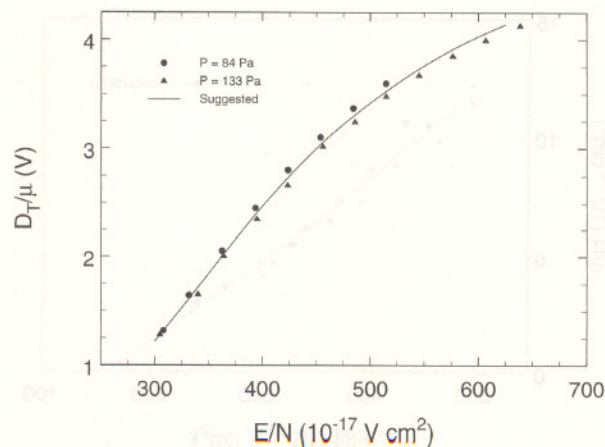


FIG. 19. Ratio of the lateral electron diffusion coefficient to electron mobility, $D_T/\mu(E/N)$, for $c\text{-C}_4\text{F}_8$ ($T = 293 \text{ K}$) from Naidu *et al.*⁷⁰

TABLE 19. Suggested values of D_T/μ (E/N) for *c*-C₄F₈ ($T=293$ K) derived from the data of Naidu *et al.*⁷⁰

E/N (10^{-17} V cm ²)	D_T/μ (E/N) (V)
300	1.22
350	1.84
400	2.47
450	3.00
500	3.42
550	3.76
600	4.03
625	4.14

9. Summary of Cross Sections and Rate Coefficients

The suggested values for the electron scattering cross sections of the *c*-C₄F₈ molecule are summarized in Fig. 20. These include values for

- (i) $\sigma_{sc,t}(\epsilon)$ from Fig. 2 and Table 4;
- (ii) $\sigma_{i,t}(\epsilon)$ from Fig. 6 and Table 9; and
- (iii) $\sigma_{a,t}(\epsilon)$ from Fig. 15(b) and Table 15

shown by the solid lines, and the lower-limit values of $\sigma_{dis,neu,t}(\epsilon)$ from Fig. 9 and Table 11 shown by the broken line.

A number of additional electron collision cross sections have been discussed in this paper, and data on these can be found as follows:

- (i) $\sigma_{e,diff}$ shown in Fig. 3 and Table 5;
- (ii) $\sigma_{i,partial}(\epsilon)$ shown in Fig. 5 and Tables 6 and 7; and
- (iii) $\sigma_{dis,partial}(\epsilon)$ shown in Fig. 9 and Table 11.

Based upon the discussions in this paper, recommended or suggested data for the electron transport coefficients, density-reduced electron attachment and ionization coefficients, and electron attachment rate constants have been presented as follows:

- (i) $k_{a,t}(\langle\epsilon\rangle)$ shown in Fig. 13 and Table 14;
- (ii) $w(E/N)$ shown in Fig. 18 and Table 18; and
- (iii) $D_T/\mu(E/N)$ shown in Fig. 19 and Table 19.

10. Data Needs

The available data on both the electron collision cross sections and the electron transport coefficients are scarce and additional measurements and calculations are required. No determination of the momentum transfer and elastic integral cross sections are available, and cross sections for other significant low-energy electron collision processes such as vi-

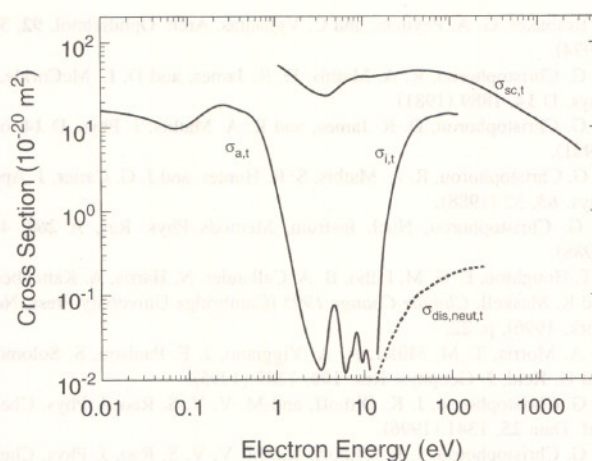


FIG. 20. Summary of suggested cross sections (see text).

brational and electronic excitation are also needed. Measurements of the electron transport coefficients over a wider range of values of the density-reduced electric field are also needed.

11. Acknowledgments

We wish to thank Professor H. Tanaka (Sophia University, Japan) for providing us with his data on the differential electron scattering cross sections. We also thank Professor J. de Urquijo (UNAM, Mexico) for providing us with his measurements on electron drift velocities and effective ionization coefficients, and Dr. C. Jiao (Air Force Research Laboratory, USA) for providing us with tables of his ionization cross sections.

12. References

- ¹J. W. Coburn, *Plasma Chem. Plasma Process.* **2**, 1 (1982).
- ²M. Miyamura, O. Tsukahoshi, and S. Komiya, *J. Vac. Sci. Technol.* **20**, 986 (1982).
- ³K. Nojiri and E. Iguchi, *J. Vac. Sci. Technol. B* **13**, 1451 (1995).
- ⁴T. Maruyama, N. Fujiwara, K. Shiozawa, and M. Yoneda, *J. Vac. Sci. Technol. A* **13**, 810 (1995).
- ⁵H. Kimura, K. Shiozawa, K. Kawai, H. Miyatake, and M. Yoneda, *Jpn. J. Appl. Phys., Part 1* **34**, 2114 (1995).
- ⁶K. Miyata, M. Hori, and T. Goto, *Jpn. J. Appl. Phys., Part 1* **36**, 5340 (1997).
- ⁷S. Samukawa and T. Mukai, *Proceedings of the International Symposium on Electron-Molecule Collisions and Swarms*, edited by Y. Hatano, H. Tanaka, and N. Kouchi, 18-20 Tokyo, Japan, July, 1999, p. 76.
- ⁸J. N. Butler, *J. Am. Chem. Soc.* **84**, 1393 (1962).
- ⁹J. M. Simmie, W. J. Quiring, and E. Tschuikow-Roux, *J. Phys. Chem.* **73**, 3830 (1969).
- ¹⁰J. M. Preses, R. E. Weston, Jr., and G. W. Flynn, *Chem. Phys. Lett.* **46**, 69 (1977).
- ¹¹M. Quack and G. Seyfang, *Ber. Bunsenges. Phys. Chem.* **86**, 504 (1982).
- ¹²E. Pochon, R. E. Weston, Jr., and G. W. Flynn, *J. Phys. Chem.* **89**, 86 (1985).
- ¹³A. Yokoyama, K. Yokoyama, and G. Fujisawa, *Chem Phys. Lett.* **237**, 106 (1995).
- ¹⁴E. W. D. Norton, *Trans. Am. Acad. Ophthalmol. Otolaryngol.* **77**, 85 (1973).

- ¹⁵ S. Brubaker, G. A. Peyman, and C. Vygantas, *Arch. Ophthalmol.* **92**, 324 (1974).
- ¹⁶ L. G. Christophorou, R. A. Mathis, D. R. James, and D. L. McCorkle, *J. Phys. D* **14**, 1889 (1981).
- ¹⁷ L. G. Christophorou, D. R. James, and R. A. Mathis, *J. Phys. D* **14**, 675 (1981).
- ¹⁸ L. G. Christophorou, R. A. Mathis, S. R. Hunter, and J. G. Carter, *J. Appl. Phys.* **63**, 52 (1988).
- ¹⁹ L. G. Christophorou, *Nucl. Instrum. Methods Phys. Res. A* **268**, 424 (1988).
- ²⁰ J. T. Houghton, L. G. M. Filho, B. A. Callander, N. Harris, A. Kattenberg, and K. Maskell, *Climate Change 1995* (Cambridge University Press, New York, 1996), p. 22.
- ²¹ R. A. Morris, T. M. Miller, A. A. Viggiano, J. F. Paulson, S. Solomon, and G. Reid, *J. Geophys. Res.* **100**, 1287 (1995).
- ²² L. G. Christophorou, J. K. Olthoff, and M. V. V. S. Rao, *J. Phys. Chem. Ref. Data* **25**, 1341 (1996).
- ²³ L. G. Christophorou, J. K. Olthoff, and M. V. V. S. Rao, *J. Phys. Chem. Ref. Data* **26**, 1 (1997).
- ²⁴ L. G. Christophorou, J. K. Olthoff, and Y. Wang, *J. Phys. Chem. Ref. Data* **26**, 1205 (1997).
- ²⁵ L. G. Christophorou and J. K. Olthoff, *J. Phys. Chem. Ref. Data* **27**, 1 (1998).
- ²⁶ L. G. Christophorou and J. K. Olthoff, *J. Phys. Chem. Ref. Data* **27**, 889 (1998).
- ²⁷ L. G. Christophorou and J. K. Olthoff, *J. Phys. Chem. Ref. Data* **28**, 131 (1999).
- ²⁸ L. G. Christophorou and J. K. Olthoff, *J. Phys. Chem. Ref. Data* **28**, 967 (1999).
- ²⁹ L. G. Christophorou and J. K. Olthoff, *J. Phys. Chem. Ref. Data* **29**, 267 (2000).
- ³⁰ L. G. Christophorou and J. K. Olthoff, *J. Phys. Chem. Ref. Data* **29**, 553 (2000).
- ³¹ J. P. Novak and M. F. Fréchet, *J. Appl. Phys.* **63**, 2570 (1988).
- ³² H. Itoh, T. Miyachi, M. Kawaguchi, Y. Nakao, and H. Tagashira, *J. Phys. D* **24**, 277 (1991).
- ³³ O. Bastiansen, O. Hassel, and L. K. Lund, *Acta Chem. Scand.* **3**, 297 (1949).
- ³⁴ H. P. Lemaire and R. L. Livingston, *J. Am. Chem. Soc.* **74**, 5732 (1952).
- ³⁵ N. V. Alekseev, I. A. Ronova, and P. P. Barzdain, *Zh. Strukt. Khim.* **9**, 1073 (1968).
- ³⁶ C. H. Chang, R. F. Porter, and S. H. Bauer, *J. Mol. Struct.* **7**, 89 (1971).
- ³⁷ N. V. Alekseev and P. P. Barzdain, *Zh. Strukt. Khim.* **15**, 181 (1972).
- ³⁸ B. Beagley, R. Calladine, R. G. Pritchard, and S. F. Taylor, *J. Mol. Struct.* **158**, 309 (1987).
- ³⁹ R. P. Bauman and B. J. Bulkin, *J. Chem. Phys.* **45**, 496 (1966).
- ⁴⁰ F. A. Miller and R. J. Capwell, *Spectrochim. Acta* **27A**, 1113 (1971).
- ⁴¹ C. Mao, C.-S. Nie, and Z.-Y. Zhu, *Spectrochim. Acta* **44A**, 1093 (1988).
- ⁴² G. Fischer, R. L. Purchase, and D. M. Smith, *J. Mol. Struct.* **405**, 159 (1997).
- ⁴³ T. M. Miller, R. A. Morris, A. E. S. Miller, A. A. Viggiano, and J. F. Paulson, *Int. J. Mass Spectrom. Ion Processes* **135**, 195 (1994).
- ⁴⁴ K. G. Mothes and R. N. Schindler, *Ber. Bunsenges. Phys. Chem.* **75**, 938 (1971).
- ⁴⁵ C. Lifshitz, T. O. Tiernan, and B. M. Hughes, *J. Chem. Phys.* **59**, 3182 (1973).
- ⁴⁶ G. K. Jarvis, K. J. Boyle, C. A. Mayhew, and R. P. Tuckett, *J. Phys. Chem. A* **102**, 3230 (1998).
- ⁴⁷ C. Lifshitz and R. Grajower, *Int. J. Mass Spectrom. Ion Phys.* **10**, 25 (1972/1973).
- ⁴⁸ M. B. Robin, *Higher Excited States of Polyatomic Molecules* (Academic, New York, 1974), Vol. I, p. 180.
- ⁴⁹ M. M. Bibby and G. Carter, *Trans. Faraday Soc.* **59**, 2455 (1963).
- ⁵⁰ L. Kevan and J. H. Futrell, *J. Chem. Soc., Faraday Trans. II* **68**, 1742 (1972).
- ⁵¹ I. Sauer, L. G. Christophorou, and J. G. Carter, *J. Chem. Phys.* **71**, 3016 (1979).
- ⁵² R. Grajower and C. Lifshitz, *Israel J. Chem.* **6**, 847 (1968).
- ⁵³ M. V. Kurepa, 3rd Cz. Conference on Electronics and Vacuum Physics Transactions, 1965, p. 107.
- ⁵⁴ P. W. Harland and J. C. J. Thynne, *Int. J. Mass Spectrom. Ion Phys.* **10**, 11 (1972/1973).
- ⁵⁵ P. W. Harland and J. L. Franklin, *J. Chem. Phys.* **61**, 1621 (1974).
- ⁵⁶ I. Ishii, R. McLaren, A. P. Hitchcock, K. D. Jordan, Y. Choi, and M. B. Robin, *Can. J. Chem.* **66**, 2104 (1988).
- ⁵⁷ J. E. Sanabia, G. D. Cooper, J. A. Tossell, and J. H. Moore, *J. Chem. Phys.* **108**, 389 (1998).
- ⁵⁸ H. Nishimura, *Proceedings of the International Symposium on Electron-Molecule Collisions and Swarms*, edited by Y. Hatano, H. Tanaka, and N. Kouchi, Tokyo, Japan, 18–20 July, 1999, p. 103.
- ⁵⁹ H. Nishimura (private communication, November 1999).
- ⁶⁰ M. Okamoto, M. Hoshino, Y. Sakamoto, S. Watanabe, M. Kitajima, H. Tanaka, and M. Kimura, *Proceedings of the International Symposium on Electron-Molecule Collisions and Swarms*, edited by Y. Hatano, H. Tanaka, and N. Kouchi, Tokyo, Japan, 18–20 July, 1999, p. 191.
- ⁶¹ H. Tanaka (private communication, 2000).
- ⁶² V. McKoy, as quoted in Ref. 61; C. Winstead and V. McKoy, *J. Chem. Phys.* **114**, 7407 (2001).
- ⁶³ H. Toyoda, M. Ito, and H. Sugai, *Jpn. J. Appl. Phys.* **36**, 3730 (1997).
- ⁶⁴ C. Q. Jiao, A. Garscadden, and P. D. Haaland, in *Gaseous Dielectrics VIII*, edited by L. G. Christophorou and J. K. Olthoff (Kluwer Academic/Plenum, New York, 1998), p. 57.
- ⁶⁵ C. Q. Jiao, A. Garscadden, and P. D. Haaland, *Chem. Phys. Lett.* **297**, 121 (1998).
- ⁶⁶ R. C. Wetzel, F. A. Baiocchi, T. R. Hayes, and R. S. Freund, *Phys. Rev.* **35**, 559 (1997).
- ⁶⁷ D. L. Smith and L. Kevan, *J. Chem. Phys.* **55**, 2290 (1971).
- ⁶⁸ J. A. Beran and L. Kevan, *J. Phys. Chem.* **73**, 3866 (1969).
- ⁶⁹ V. Tarnovsky and K. Becker, *J. Chem. Phys.* **98**, 7868 (1993).
- ⁷⁰ M. S. Naidu, A. N. Prasad, and J. D. Craggs, *J. Phys. D* **5**, 741 (1972).
- ⁷¹ T. Tagashira, Y. Miyamoto, and M. Shimozuma, *Proceedings of the XVIII International Conference on Phenomena in Ionized Gases*, Swansea, U. K., 13–17 July, 1987, p. 680.
- ⁷² C. Wen and J. M. Wetzer, IX International Conference on Gas Discharges and their Applications, Venezia, Italy, 19–23 September, 1988, p. 367.
- ⁷³ J. de Urquijo (private communication, July 2000); J. de Urquijo and E. Basurto, *J. Phys. D* **34**, 1352 (2001).
- ⁷⁴ J. Berril, M. J. Christensen, and I. W. McAllister, in *Gaseous Dielectrics V*, edited by L. G. Christophorou and D. W. Bouldin (Pergamon, New York, 1987), p. 304.
- ⁷⁵ L. G. Christophorou, R. A. Mathis, S. R. Hunter, and J. G. Carter, in *Gaseous Dielectrics V*, edited by L. G. Christophorou and D. W. Bouldin (Pergamon, New York, 1987), p. 88.
- ⁷⁶ H. Kazumi, R. Hamasaki, and K. Tago, *Plasma Sources Sci. Technol.* **5**, 200 (1996).
- ⁷⁷ L. G. Christophorou, D. L. McCorkle, and A. A. Christodoulides, in *Electron-Molecule Interactions and Their Applications*, edited by L. G. Christophorou (Academic, New York, 1984), Vol. 1, Chap. 6.
- ⁷⁸ W. T. Naff, C. D. Cooper, and R. N. Compton, *J. Chem. Phys.* **49**, 2784 (1968).
- ⁷⁹ J. M. S. Henis and C. A. Mabie, *J. Chem. Phys.* **53**, 2999 (1970).
- ⁸⁰ R. L. Woodin, M. S. Foster, and J. L. Beauchamp, *J. Chem. Phys.* **72**, 4223 (1980).
- ⁸¹ L. G. Christophorou, *Adv. Electron. Electron Phys.* **46**, 55 (1978).
- ⁸² A. Chutjian and S. H. Alajajian, *J. Phys. B* **20**, 839 (1987).
- ⁸³ A. A. Christodoulides, L. G. Christophorou, R. Y. Pai, and C. M. Tung, *J. Chem. Phys.* **70**, 1156 (1979).
- ⁸⁴ R. M. Reese, V. H. Dibeler, and F. L. Mohler, *J. Res. Nat. Bur. Stand.* **57**, 367 (1956).
- ⁸⁵ A. Kono and K. Kato, *Appl. Phys. Lett.* **77**, 495 (2000).
- ⁸⁶ S. M. Spyrou, S. R. Hunter, and L. G. Christophorou, *J. Chem. Phys.* **83**, 641 (1985).
- ⁸⁷ L. G. Christophorou, D. L. McCorkle, and D. Pittman, *J. Chem. Phys.* **60**, 1183 (1974).
- ⁸⁸ A. A. Christodoulides, L. G. Christophorou, and D. L. McCorkle, *Chem. Phys. Lett.* **139**, 350 (1987).
- ⁸⁹ E. Schultes, Ph.D. dissertation, University of Bonn, 1973; as quoted in Ref. 90.
- ⁹⁰ A. A. Christodoulides, E. Schultes, R. Schumacher, and R. N. Schindler, *Z. Naturforsch.* **29a**, 389 (1974).
- ⁹¹ F. J. Davis, R. N. Compton, and D. R. Nelson, *J. Chem. Phys.* **59**, 2324 (1973).

- ⁹²K. M. Bansal and R. W. Fessenden, *J. Chem. Phys.* **59**, 1760 (1973).
- ⁹³L. G. Christophorou and P. G. Datskos, *Int. J. Mass Spectrom. Ion Processes* **149/150**, 59 (1995).
- ⁹⁴M. Yamaji, Y. Okada, and Y. Nakamura, *Proceedings of the International Symposium on Electron-Molecule Collisions and Swarms*, edited by Y. Hatano, H. Tanaka, and N. Kouchi, Tokyo, Japan, 18–20 July 1999, p. 151.
- ⁹⁵T. Su and L. Kevan, *J. Phys. Chem.* **77**, 148 (1973).
- ⁹⁶R. A. Morris, A. A. Viggiano, S. T. Arnold, and J. F. Paulson, *Int. J. Mass Spectrom. Ion Processes* **149/150**, 287 (1995).

